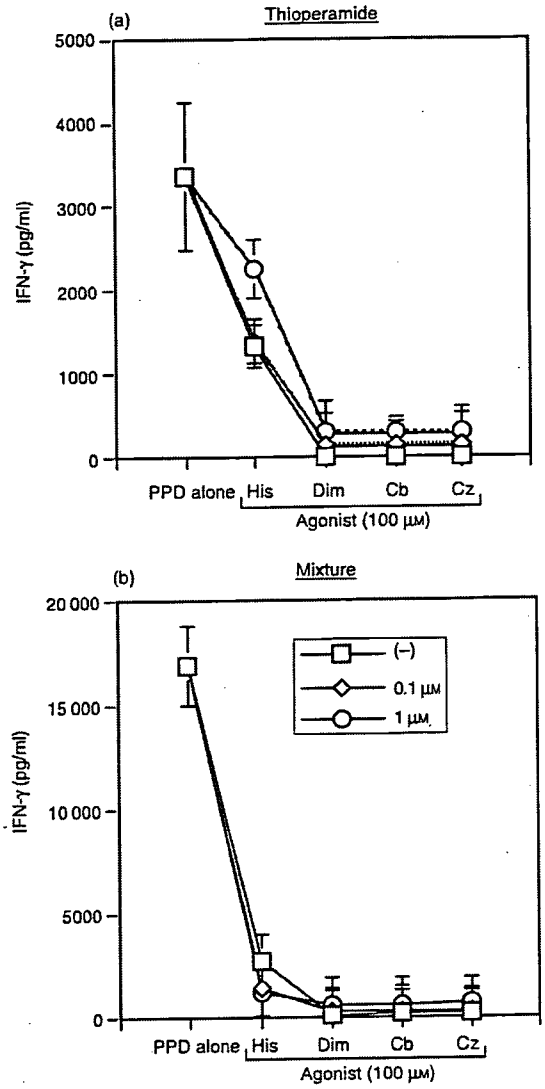

Figure 5. Effect of histamine receptor (HR)-selective antagonists on the inhibition of interferon-γ (IFN-γ) production induced by H4R-selective agonists. Peripheral blood mononuclear cells (PBMCs) were pretreated for 30 min with thioperamide (a) or with a mixture of antagonists (b) at the following concentrations: (a) pretreatment with 0 μM (square), 0·1 μM (diamond) or 1·0 μM (circle) thioperamide; (b) simultaneous pretreatment with each concentration of 0 μM (square), 0·1 μM (diamond) or 1·0 μM (circle) *d*-chlrophenirамine, famotidine and thioperamide. Then, cells were incubated with 2 μg/ml of purified protein derivative of *Mycobacterium tuberculosis* (PPD) and 100 μM histamine (His), dimaprit (Dim), clobenpropit (Cb), or clozapine (Cz). Results are presented as the mean concentrations ± standard deviation (SD) from triplicate cultures. Data are representative of three separate experiments.

Role of adenylate cyclase and apoptosis in histamine suppression of PPD-induced IFN-γ production

We examined whether the inhibition by histamine and H4R-selective agonists depends on the activity of adenylate cyclase. Pretreatment of PBMCs with SQ22536, an adenylate cyclase inhibitor, reversed the inhibition of PPD-induced IFN-γ production by histamine and dimaprit. Furthermore, pretreatment with RP-8-Br-cAMPS, a PKA type 1 inhibitor, completely reversed the inhibition by histamine and dimaprit (Fig. 6a,b). Pretreatment of PBMC with SQ22536 and RP-8-Br-cAMPS also reversed the inhibition by clozapine (Fig. 6d), but the effects were weaker than observed for the reversal of inhibition by histamine. However, a minimal effect of SQ22536 and RP-8-Br-cAMPS was seen on the effect of clopenpropit (Fig. 6c). These results were seen in both high and low responders for PPD-induced IFN-γ production (data not shown). The addition of SQ22536 or RP-8-Br-cAMPS had no effect on the IFN-γ production by PBMCs in response to PPD alone (data not shown).

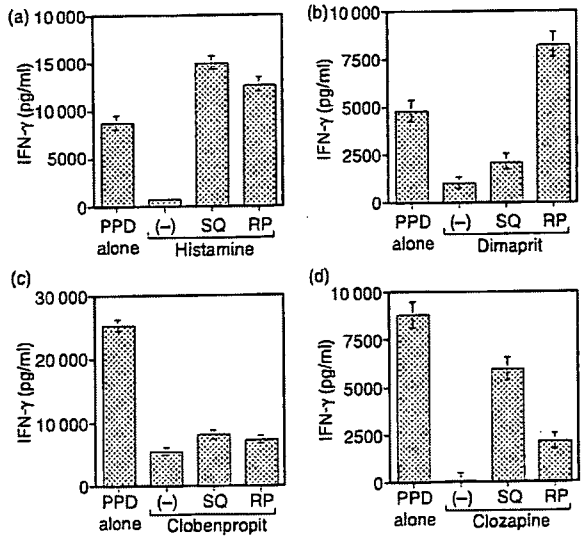

Figure 6. Roles of cAMP and protein kinase A (PKA) in the inhibition of purified protein derivative of *Mycobacterium tuberculosis* (PPD)-induced interferon-γ (IFN-γ) production by H4R-selective agonists. Peripheral blood mononuclear cells (PBMCs) were pretreated for 60 min with SQ22536 (SQ) or RP-8-Br-cAMPS (RP) and then incubated with 2 μg/ml of PPD and 100 μM histamine (a), dimaprit (b), clobenpropit (c), or clozapine (d). The results are expressed as the mean concentrations ± standard deviation (SD) from triplicate cultures. Data are representative of three separate experiments.

Pretreatment of PPD-specific TCLs alone with SQ22536, followed by coculture with intact APCs, partially suppressed inhibition of the PPD-specific IFN-γ production by dimaprit. Similar suppression was observed when APCs alone were pretreated with SQ22536, followed by the coculture with intact TCLs. However, pretreatment of both TCLs and APCs with SQ22536 markedly reversed the inhibitory effects of dimaprit on the PPD-specific response (Fig. 7).

The addition of 100 μM dimaprit, clobenpropit, or clozapine, but not of histamine, induced annexin-V expression on PBMCs (Fig. 8). $CD19^+$ cells were highly

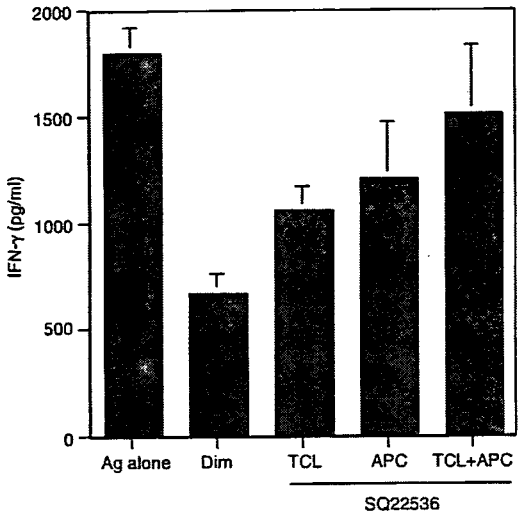

Figure 7. Reversal of H4R-selective agonist-induced inhibition of antigen (Ag)-specific T-cell responses with an adenylate cyclase inhibitor. Purified protein derivative of a *Mycobacterium tuberculosis* (PPD)-specific T-cell line (TCL) alone, antigen-presenting cells (APCs) alone, or both TCL and APC, were pretreated with SQ22536 at 37° for 1 hr. Following incubation, the cells were washed with culture medium three times, after which they were mixed and cultured with the PPD, in the presence of 100 μM dimaprit (Dim), for 65 hr. Data are representative of two separate experiments.

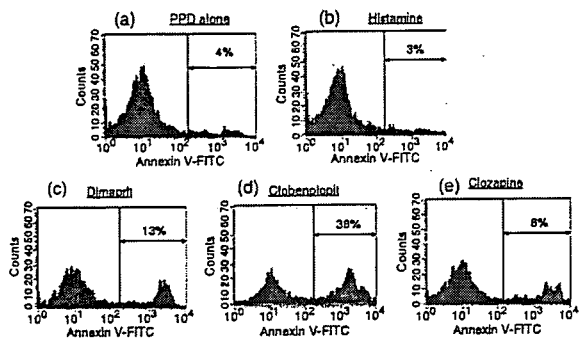

Figure 8. Expression of annexin-V by peripheral blood mononuclear cells (PBMCs) following treatment with H4R-selective agonists. PBMCs were incubated for 72 hr with purified protein derivative of *Mycobacterium tuberculosis* (PPD) (a) and histamine (b), dimaprit (c), clobenpropit (d), or clozapine (e), and the expression of annexin-V on $CD19^+$ cells was analysed by flow cytometry. Data are representative of six separate experiments.

susceptible to the induction of annexin-V expression following exposure to H4R-related agonists. H4R agonists also induced annexin-V expression in $CD4^+$ cells, but not in $CD8^+$ cells (data not shown).

cDNA miroarray analysis

We sought to compare the comprehensive expression of mRNA in PBMC following PPD stimulation in the presence or absence of clozapine. Among 16 600 genes tested, the amounts of mRNA were unchanged in 96·2% of the genes. However, the mRNA levels of 0·8% of the genes (such as melanocortin 1 receptor) were increased (> 200%) in the presence of clozapine. On the contrary, the mRNA levels of 3·0% of the genes, such as IFN-γ, were decreased (< 50%) (Table 1).

Effect of HR-selective agonists on Cry j1-induced IL-5 production

We examined the effect of HR-selective agonists on human Th2 responses. PBMCs from patients with Japanese cedar pollinosis produced a comparable amount of IL-5 in response to Cry j1. The addition of 100 μM 2-PEA, 4-MH or α-MH displayed no significant effect on Cry j1-induced IL-5 production. However, H4R agonists, including dimaprit, clobenpropit and clozapine, significantly inhibited Cry j1-induced IL-5 production (Fig. 9).

Expression of the four histamine receptors on Ag-specific TCLs

Finally, mRNA expression of the four histamine receptors was examined in five PPD- and five Cry j1-specific TCLs by reverse transcription–polymerase chain reaction (RT–PCR). H3R mRNA expression was completely undetectable in all TCLs. On the other hand, H1R, H2R and H4R mRNA were clearly detected in most TCLs (Fig. 10). Using real-time PCR analysis, relative expression levels of the four HRs were not observed to differ significantly among Cry j1- and PPD-specific TCLs (H1R, $P = 0{\cdot}117$; H2R, $P = 0{\cdot}245$; H4R, $P = 0{\cdot}344$; using the Mann–Whitney *U*-test). The expression levels of H4R in TCLs were lower than that of H1R; however, significantly increased expression of the H4R was observed as compared to H2R and H3R (Fig. 11).

Discussion

In the present study, we demonstrated that histamine inhibits PPD-induced IFN-γ production in PBMCs. Several studies have investigated the regulatory role of histamine on IFN-γ production by T cells.[7,8,14–16] Lagier *et al.* reported that histamine inhibits IFN-γ production by human Th1-like T-cell clones (TCCs) specific for *Dermatophagoides pteronyssinus*, whereas it did not have a significant inhibitory effect on T helper 0 (Th0)-like TCCs, and it had no effect on Th2-like TCCs stimulated with phorbol 12-myristate 13-acetate (PMA) and a calcium ionophore.[8] Krouwels *et al.* reported that histamine inhibited IFN-γ production in 21 out of 52 human TCCs (40%), whereas IFN-γ production was enhanced in eight of the TCCs (16%). Also, histamine did not affect IFN-γ production in 23 TCCs (44%) in response to plate-bound

Table 1. Ranked list of up-regulated and down-regulated transcripts in purified protein derivative of *Mycobacterium tuberculosis* (PPD)-stimulated peripheral blood mononuclear cells with clozapine

	Up-regulated transcripts				Down-regulated transcripts		
Rank	Gene name	GenBank acc. no.	Ratio[1]	Rank	Gene name	GenBank acc. no.	Ratio[1]
1	Melanocortin 1 receptor	NM_002386	8·50	1	Interferon-γ	NM_000619	0·02
2	LOC90271	XM_030445	5·59	2	Chemokine (C-C motif) ligand 5	NM_002981	0·02
3	ATP-binding cassette, subfamily G (WHITE) member 1, transcript variant 1	NM_004915	4·75	3	Matrix metalloproteinase 10	NM_002425	0·02
4	Actin-binding LIM protein 2	NM_032432	4·69	4	Chemokine (C-X-C motif) ligand 5	NM_002994	0·03
5	Liver-expressed antimicrobial peptide 2	NM_052971	4·32	5	KIAA1046 protein	NM_014928	0·03
6	Oviductal glycoprotein 1, 120 000 MW	NM_002557	4·30	6	Secreted phosphoprotein 1	NM_000582	0·03
7	Killer-specific secretory protein of 37 000 MW	NM_031950	3·96	7	Chemokine (C-X-C motif) ligand 1	NM_001511	0·03
8	LOC286006	XM_209854	3·83	8	Tumor necrosis factor (ligand) superfamily member 15	NM_005118	0·03
9	Myelin-basic protein	NM_002385	3·73	9	Similar to immune-responsive protein 1	XM_292184	0·04
10	Hypothetical protein LOC157562	XM_098779	3·71	10	Matrix metalloproteinase 7	NM_002423	0·04

[1]Ratio: with clozapine versus without clozapine.
GenBank acc. no., GenBank accession number; MW, molecular weight.

anti-CD3 mAb.[14] In contrast, pretreatment with histamine does enhance IFN-γ production in response to plate-bound anti-CD3 mAb in human Th1 cells.[7] Furthermore, Osna *et al.* showed that the effect of histamine on IFN-γ production was dependent on the stimulatory signals.[15]

We investigated the PPD-induced human T-cell responses to clarify whether histamine affects antigen-specific T-cell responses. Our results are consistent with previous reports. Osna *et al.* reported that histamine up-regulates IL-10 production in murine splenocytes and inhibits IFN-γ production.[16] In the current study, PBMCs did not produce IL-10 in response to PPD, and IL-10 production was not induced in the presence of histamine, suggesting that factors other than IL-10 may be involved in the inhibitory effect of histamine.

The H4R agonists dimaprit, clobenpropit and clozapine all eliminated PPD-induced proliferation and IFN-γ production in PBMCs. H4R is selectively expressed in cells of haematopoietic lineage, including mast cells, eosinophils and lymphocytes.[3,17] Physiological roles of H4R in mast cells, eosinophils, neutrophils and dendritic cells have been implied in recent years, but whether signals through H4R can affect T-cell functions has not been determined.[6,17–19] One report demonstrated that histamine induces IL-16 production by human $CD8^+$ T cells through H2R and H4R.[9] Our results, using HR-related agonists, suggest that signals through H4R may exert an inhibitory role on antigen-specific T-cell responses. However, thioperamide, an H3R and H4R antagonist, did not reverse the inhibition of PPD-induced IFN-γ production by either histamine or H4R agonists. Thioperamide, *d*-chlorpheniramine and famotidine, the HR antagonists used in the present study, were confirmed to be functional in previous studies.[20,21] This suggests that the inhibitory effect of histamine and H4R agonists is not mediated by H4R. In addition, a mixture of *d*-chlrpheniramine, famotidine and thioperamide did not reverse the inhibition by histamine, suggesting that the effect is independent of H1R, H2R and H3R/H4R.

2-PEA, an H1R-selective agonist, did not affect PPD-induced IFN-γ production. On the other hand, 4-MH, an H2R-selective agonist, partially inhibited its production. It is known that histamine regulates cytokine production, via H2R, on T cells.[8,14,15,22] In addition, histamine inhibits IL-12 production by monocytes via H2R.[23] Our finding that dimaprit, an H2R and H4R agonist, inhibited PPD-induced IFN-γ production, suggests that signals through H2R may be involved in the inhibition. However, the inhibitory effect of either histamine or dimaprit

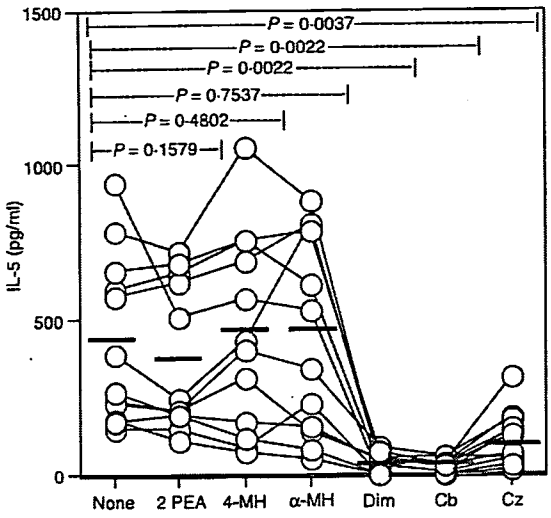

Figure 9. Histamine receptor (HR)-selective agonists-mediated inhibition of Cry j1-specific interleukin (IL)-5 production by peripheral blood mononuclear cells (PBMCs). PBMCs from 12 patients with Japanese cedar pollinosis were cultured with 10 μg/ml of Cry j1, in the presence or absence of 2-pyridylethylamine (2-PEA), 4-methylhistamine (4-MH), alpha-methylhistamine (α-MH), dimaprit (Dim), clobenpropit (Cb) or clozapine (Cz), at 100 μM, for 72 hr. Following incubation, supernatant was collected and the concentrations of IL-5 were determined in each sample using an enzyme-linked immunosorbent assay (ELISA). *P*-values were obtained using Wilcoxon's signed-rank test.

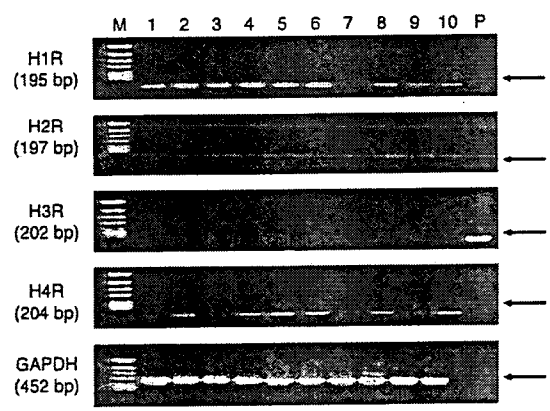

Figure 10. Expression of four histamine receptors (HRs) by human T-cell lines (TCLs). mRNA was extracted from five Cry j1-specific TCLs (lanes 1–5) and from five purified protein derivative of *Mycobacterium tuberculosis* (PPD)-specific TCLs (lanes 6–10), after which the levels of H1R, H2R, H3R, H4R and glyceraldehyde 3-phosphate dehydrogenase (GAPDH) were detected by reverse transcription–polymerase chain reaction (RT–PCR), as described in the Materials and methods. M, molecular marker; P, positive control (NEC14).

was not reversed by famotidine, suggesting that H2R signalling had a negligible role in the inhibition of PPD-induced IFN-γ production.

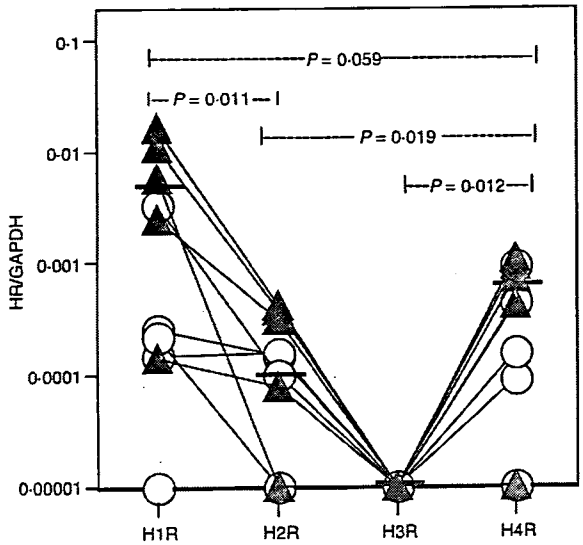

Figure 11. Comparison of the amounts of four histamine receptors (HRs) among T-cell lines (TCLs). The expression levels of four HRs were determined in five Cry j1-specific TCLs (closed triangle) and in five purified protein derivative of *Mycobacterium tuberculosis* (PPD)-specific TCLs (open circle) using real-time reverse transcription–polymerase chain reaction (RT–PCR). Each bar represents the median expression level of each messenger. *P*-values were obtained using Wilcoxon's signed-rank test.

The pretreatment of PBMCs with SQ22536, an adenylate cyclase inhibitor, and with RP-8-Br-cAMPS, a PKA type 1 inhibitor, reversed the inhibition of PPD-induced IFN-γ production by histamine and H4R agonists. Previous reports demonstrated that 5 mM SQ22536 and 5 mM RP-8-Br-cAMPS reversed, almost completely, the inhibitory effect of several compounds on human PBMC responses.[12] These results suggest that H4R agonists, except for clobenpropit, inhibit PPD-induced IFN-γ production by elevating intracellular cAMP levels and activating PKA. Moreover, results using PPD-specific TCLs and APCs suggest that H4R agonists may influence PPD-specific cellular responses at both the T-cell and APC level. It is known that H2R activation causes an elevation of the intracellular cAMP level.[24] In addition, PKA plays a pivotal role in histamine-mediated regulation of IFN-γ production, especially via the stimulation of T-cell receptors.[15] Although dimaprit can act as an H2R agonist, clozapine and clobenpropit cannot.[25] H4R is coupled to $G_{i/o}$, which leads to the inhibition of cAMP formation.[26] This further supports the possibility that the inhibitory effect of H4R agonists is not associated with typical H4R signaling. Rather, signals similar to those mediated by H2R may participate in the inhibition. However, we also observed that the inhibitory effect of either histamine or dimaprit was not reversed by famotidine, suggesting that H2R signaling had a negligible role in the inhibition of PPD-induced IFN-γ production. In addition, the varied effect of SQ22536 and RP-8-Br-cAMPS on IFN-γ

production induced by different agonists may suggest the presence of unidentified pleural receptors in the action of agonists.

$CD19^+$ and $CD4^+$ cells express annexin-V following exposure to H4R agonists, suggesting that these compounds induce apoptosis in these cells. On the other hand, cDNA microarray analysis revealed that the changes of mRNA levels were seen in 0·8% of the genes tested, such as melanocortin 1 receptor, following the stimulation with H4R agonist (Table 1), indicating that the inhibitory effects of H4R agonists were not non-specific or solely the result of an apoptotic effect. For example, melanocortin 1 receptor has signal transducer activity and it is involved in immunosuppression.[27] Thus, the suppressive role of H4R agonists may be associated with the activation of melanocortin 1 receptor. In addition, histamine did not induce the expression of annexin-V. These results suggest that the inhibitory effect of H4R agonists is not associated with the binding to classical HRs.

Concentrations of histamine and H4R agonists ranging from 10^{-5} to 10^{-4} M displayed a dose-dependent inhibition of PPD-induced IFN-γ production by PBMCs. Although it was difficult to define precisely the histamine concentration in the target organ, concentrations of histamine from 10^{-6} to 10^{-4} M have been reported to be comparable to those measured in tissues after mast cell degranulation.[28]

In conclusion, we examined the effect of histamine and H4R agonists on antigen-specific human T-cell responses. H4R signaling is important for functions of other immune cells, such as mast cell chemotaxis, eosinophil chemotaxis and suppression of IL-12 production by dendritic cells.[3,29] H4R agonists inhibit Ag-specific cytokine production; however, our investigations, using antagonists of H4R and inhibitors of adenylate cyclase or PKA, revealed that H4R plays a negligible role in the inhibition. These results indicate that there may be a previously unidentified HR or receptor subtype that can bind to dimaprit, clobenpropit and clozapine and that can mediate the inhibition of antigen-induced cellular responses via a cAMP/PKA-dependent, apoptotic pathway. More recently, Lim *et al.* have reclassified 4-MH as the most selective H4R agonist so far at the H4R.[30] This seems to be relevant for understanding the present results, suggesting a new orphan receptor. Furthermore, our observations may provide the basis for novel therapeutic approaches in the management of allergic and autoimmune diseases.

Acknowledgements

The authors would like to thank Yuko Okano for her editorial assistance. This work was supported, in part, by grants from Research on Allergic disease and Immunology of Ministry of Health, Labor and Welfare (no. 14210301 to MO).

References

1 Akdis CA, Simons FER. Histamine receptors are hot in immunopharmacology. *Eur J Pharmacol* 2006; 533:69–76.
2 Oda T, Morikawa N, Saito Y, Masuho Y, Matsumoto S. Molecular cloning and characterization of a novel type of histamine receptor preferentially expressed in leukocytes. *J Biol Chem* 2000; 275:36781–6.
3 de Esch IJP, Thurmond RL, Jongejan A, Leurs R. The histamine H4 receptor as a new therpeutic target for inflammation. *Trends Pharmacol Sci* 2005; 26:462–9.
4 Ling P, Ngo K, Nguyen S, Thurmond RL, Edwards JP, Karlsson L, Fung-Leung W. Histamine H4 receptor mediates eosinophil chemotaxis with cell shape change and adhesion molecule upregulation. *Br J Pharmacol* 2004; 142:161–71.
5 O'Reilly M, Alpert R, Jenkinson S *et al.* Identification of a histamine H4 receptor on human eosinophils – role in eosinophil chemotaxis. *J Recept Signal Transduct Res* 2002; 22:431–48.
6 Gutzmer R, Diestel C, Mommert S, Kother B, Stark H, Wittmann M, Werfel T. Histamine H4 receptor stimulation suppresses IL-12p70 production and mediates chemotaxis in human monocyte-derived dendritic cells. *J Immunol* 2005; 174:5224–32.
7 Jutel M, Watanabe T, Klunker S *et al.* Histamine regulated T-cell and antibody responses by differential expression of H1 and H2 receptors. *Nature* 2001; 413:420–5.
8 Lagier B, Lebel B, Bousquet J, Pene J. Different modulation by histamine of IL-4 and interferon-gamma (IFN-γ) release according to phenotype of human Th0, Th1, Th2 clones. *Clin Exp Immunol* 1997; 108:545–51.
9 Gantner F, Sakai K, Tusche MW, Cruikshank WW, Center DM, Bacom KB. Histamine H4 and H2 receptors control histamine-induced interleukin-16 release from human CD8+ T cells. *J Pharmacol Exp Ther* 2002; 303:300–7.
10 Okano M, Sugata Y, Fujiwara T *et al.* E prostanoid 2 (EP2)/EP4-mediated suppression of antigen-specific human T cell responses by prostaglandin E2. *Immunology* 2006; 118:343–52.
11 Okano M, Kino K, Takishita T, Hattori H, Ogawa T, Yoshino T, Yokoyama M, Nishizaki K. Roles of carbohydrates on Cry j 1, the major allergen of Japanese cedar pollen, in specific T-cell responses. *J Allergy Clin Immunol* 2001; 108:101–8.
12 Aandahl EM, Moretto WJ, Haslett PA, Vang T, Bryn T, Tasken K, Nixon DF. Inhibition of antigen-specific T cell proliferation and cytokine production by protein kinase A Type I. *J Immunol* 2002; 169:802–8.
13 Motoyama T, Watanabe H, Yamamoto T, Sekiguchi M. Human testicular germ cell tumors *in vitro* and in athymic nude mice. *Acta Pathol Jpn* 1987; 37:431–48.
14 Krouwels FH, Hol BEA, Lutter R, Bast A, Jansen HM, Out TA. Histamine affects interleukin-4, and interferon-γ production by human T cell clones from the airways and blood. *Am J Respir Cell Mol Biol* 1998; 18:721–30.
15 Osna N, Elliott K, Khan MM. The effects of histamine on interferon gamma production are dependent on the stimulatory signals. *Int Immunopharmacol* 2001; 1:135–45.
16 Osna N, Elliott K, Khan MM. Regulation of interleukin-10 secretion by histamine in TH2 cells and splenocytes. *Int Immunopharmacol* 2001; 1:85–96.
17 Liu C, Ma X, Jiang X, Wilson SJ *et al.* Cloning and pharmacological characterization of a fourth histamine receptor (H4) expressed in bone marrow. *Mol Pharamcol* 2001; 59:420–6.

18 Buckland KF, Williams TJ, Conroy DM. Histamine induces cytoskeletal change in human eosinophils via the H4 receptor. *Br J Pharmacol* 2003; 140:1117–27.

19 Takeshita K, Sakai K, Bacon KB, Gantner F. Critical role of histamine H4 receptor in leukotriene B4 production and mast cell-dependent neutrophil recruitment induced by zymosan *in vivo*. *J Pharmacol Exp Ther* 2003; 307:1072–8.

20 Ito Y, Oishi R, Nishibori M, Saeki K. Characterization of histamine release from the rat hypothalamus as measured by *in vivo* microdialysis. *J Neurochem* 1991; 56:769–74.

21 Yokoyama M, Yokoyama A, Mori S *et al.* Inducible histamine protects mice from *P. acnes*-primed and LPS-induced hepatitis through H2-receptor stimulation. *Gastroenterology* 2004; 127:892–902.

22 Poluektova LY, Khan MM. Protein kinase A inhibitors reverse histamine-mediated regulation of IL-5 secretion. *Immunopharmacology* 1998; 39:9–19.

23 Elenkov IJ, Webster E, Panicolaou DA, Fleisher TA, Chrousos GP, Wilder RL. Histamine potently suppresses human IL-12 and stimulates IL-10 production via H2 receptors. *J Immunol* 1998; 161:2586–93.

24 Gantz I, Munzert G, Tashiro T, Schaffer M, Wang L, Delvalle J, Yamada T. Molecular cloning of human histamine H2 receptor. *Biochem Biophys Res Commun* 1991; 178:1386–92.

25 Hough LB. Genomics meets histamine receptors: new subtypes, new receptors. *Mol Pharmacol* 2001; 59:415–9.

26 Nakamura T, Itadani H, Hidaka Y, Ohta M, Tanaka K. Molecular cloning and characterization of a new human histamine receptors, HH4R. *Biochem Biophys Res Commun* 2000; 279:615–20.

27 Cooper A, Robinson SJ, Rickard C, Jackson CL, Friedmann PS, Healy E. Alpha-melanocyte-stimulating hormone suppresses antigen-induced lymphocyte stimulation in humans independently of melanocortin 1 receptor gene status. *J Immunol* 2005; 175:4806–13.

28 Jeannin P, Delneste Y, Gosset P, Molet S, Lassale P, Hamid Q, Tsicopoulos A, Tonnel AB. Histamine induces interleukin-8 secretion by endothelial cells. *Blood* 1994; 84:2229–33.

29 Hofstra CL, Desai PJ, Thurmond RL, Fung-Leung WP. Histamine H4 receptor mediates chemotaxis and calcium mobilization of mast cells. *J Pharmacol Exp Ther* 2003; 305: 1212–21.

30 Lim HD, van Rijin RM, Ling P, Bakker RA, Thurmond RL, Leurs R. Evaluation of histamine H1-, H2-, and H3-receptor ligands at the human histamine H4 receptor: identification of 4-methylhistamine as the first potent and selective H4 receptor agonist. *J Pharmacol Exp Ther* 2005; 314:1310–21.

Biosci. Biotechnol. Biochem., 72, 70572-1–7, 2008

Glycoform Analysis of Japanese Cypress Pollen Allergen, Cha o 1: A Comparison of the Glycoforms of Cedar and Cypress Pollen Allergens

Yoshinobu KIMURA,[1,2,†] Misao KUROKI,[2] Megumi MAEDA,[1,*] Mitsuhiro OKANO,[3] Minehiko YOKOYAMA,[4] and Kosuke KINO[4]

[1]*Department of Biofunctional Chemistry, Graduate School of Natural Science and Technology, Okayama University, 1-1-1 Tsushima-Naka, Okayama 700-8530, Japan*
[2]*Department of Bioresources Chemistry, Faculty of Agriculture, Okayama University, 1-1-1 Tsushima-Naka, Okayama 700-8530, Japan*
[3]*Department of Otolaryngology-Head and Neck Surgery, Okayama University, Graduate School of Medicine and Dentistry, Okayama 700-8558, Japan*
[4]*Meiji Co., Odawara 250-0862, Japan*

Received September 5, 2007; Accepted October 18, 2007; Online Publication, February 7, 2008
[doi:10.1271/bbb.70572]

A Japanese cypress (*Chamaecyparis obtusa*) pollen allergen, Cha o 1, is one of the major allergens that cause allergic pollinosis in Japan. Although it has been found that Cha o 1 is glycosylated and that the amino acid sequence is highly homologous with that of Japanese cedar pollen allergen, the structure of *N*-glycans linked to Cha o 1 remains to be determined. In this study, therefore, we analyzed the structures of the *N*-glycans of Cha o1. The *N*-glycans were liberated by hydrazinolysis from purified Cha o 1, and the resulting sugar chains were *N*-acetylated and pyridylaminated. The structures of pyridylaminated *N*-glycans were analyzed by a combination of exoglycosidase digestion, two dimensional (2D-) sugar chain mapping, and electrospray ionization mass spectrometry analysis. Structural analysis indicated that the major *N*-glycan structure of Cha o1 is GlcNAc2Man3Xyl1Fuc1GlcNAc2 (89%), and that high-mannose type structures (Man9-GlcNAc2, Man7GlcNAc2) occur as minor components (11%).

Key words: *N*-glycan structure; antigenic oligosaccharide; Japanese cypress pollen allergen; Cha o 1; *Chamaecyparis obtusa*

In previous studies,[1,2] we determined the chemical structures of *N*-glycans linked to two cedar pollen allergens, Cry j 1 (Japanese cedar pollen allergen) and Jun a 1 (mountain cedar pollen allergen), and revealed that biantennary plant complex type *N*-glycans harboring Lewis a epitope occur in their *N*-glycan moieties. This finding suggests that the Lewis a epitope may play a critical role in pollinosis, but the occurrence of this epitope in plant glycoallergens has been reported from only three pollen allergens, Cup a 1 (pollen allergen from Arizona cypress),[3] Cry j 1, and Jun a 1. Japanese cypress pollen is another major allergic pollen in Japan, and Cha o 1 is a major allergen contained in the cypress pollens. Although it is known that Cha o 1 is *N*-glycosylated,[4] the detailed chemical structures of the *N*-glycan moiety remain to be determined. Hence, in this study, we analyzed the structures of *N*-glycans linked to the Japanese cypress pollen allergen Cha o 1 to determine whether plant specific antigenic oligosaccharide or Lewis a epitope occurs in the allergen. First, we purified Cha o 1 from an extract of the cypress pollens by a combination of ion-exchange chromatography and gel-filtration, using an antiserum against Cha o 1 to monitor the elution position of the allergen. We found that Cha o 1 occured in two forms, with the same N-terminal amino acid sequence but different molecular weights, suggesting that the numbers of the *N*-glycosylation sites might be different from each other. Furthermore, structural analysis of *N*-glycans revealed

† To whom correspondence should be addressed. Fax: +81-86-251-8388; E-mail: yosh8mar@cc.okayama-u.ac.jp
* Present address: *Department of Hygiene, Kawasaki Medical School, 577 Matsushima, Kurashiki 701-0192, Japan*

Abbreviations: PA-, pyridylamino; RP-HPLC, reverse-phase HPLC; SF-HPLC, size-fractionation HPLC; ESI-MS, electrospray ionization mass spectrometry; CBB, Coomassie Brilliant Blue; Hex, hexose; HexNAc, *N*-acetylhexosamine; Deoxyhex, deoxyhexose; Pen, pentose; M3FX, Manα1-6(Manα1-3)(Xylβ1-2)Manβ1-4GlcNAcβ1-4(Fucα1-3)GlcNAc-PA; MFX, Xylβ1-2Manβ1-4GlcNAcβ1-4(Fucα1-3)GlcNAc-PA; GN2M3FX, GlcNAcβ1-2Manα1-6(GlcNAcβ1-2Manα1-3)(Xylβ1-2)Manβ1-4GlcNAcβ1-4(Fucα1-3)GlcNAc-PA; M9A, Manα1-2Manα1-6(Manα1-2Manα1-3)-Manα1-6(Manα1-2Manα1-2Manα1-3)Manβ1-4GlcNAcβ1-4GlcNAc-PA; M7A, Manα1-2Manα1-6(Manα1-3)Manα1-6(Manα1-2Manα1-3)Manβ1-4GlcNAcβ1-4GlcNAc-PA

that Cha o 1 bears both a biantennary complex type and a high-mannose type oligosaccharide. The predominant occurrence of the antigenic plant complex type structure, GlcNAc2Man3Xyl1Fuc1GlcNAc2 (GN2M3FX), is a characteristic common to allergenic pollen glycoproteins.[1-3] But the Lewis a unit was not found in the *N*-glycans of Cha o 1, in contrast with Cup a 1, Cry j 1, and Jun a 1, indicating that the Lewis a epitope is not involved in the symptoms of pollinosis.

Materials and Methods

Materials. An Asahipak NH2P-50 4E column (0.46 × 25 cm) was purchased from Showa Denko (Tokyo, Japan), and a Cosmosil 5C18-AR column (0.6 × 25 cm) from Nacalai Tesque (Kyoto, Japan). GN2M3FX were prepared from glycoproteins from rice culture cells.[5] M7A and M9A were prepared from royal jelly glycoproteins.[6] Antiserum against Cha o 1 was a generous gift of Meiji Co. Antiserum against β1-2 xylose-containing *N*-glycans was a generous gift of Dr. Arnd Strum (Friedrich-Miescher Institute, Basel, Switzerland).[7]

Purification of Cha o 1. Purification of Cha o 1 was basically done as described in a previous paper.[4] During the purification steps, the elution of Cha o 1 was monitored by immunoblotting assay using antiserum against Cha o 1. Japanese cypress pollen (100 g) was defatted in acetone (500 ml), and the resulting defatted pollen was suspended in 125 mM $(NH_4)_2CO_3$ and sonicated in an ice bath for 5 min. After incubation for 16 h at 4 °C, the extract was centrifuged at 8,000 rpm for 20 min, and the resulting supernatant was 80% saturated with ammonium sulfate. The protein precipitate was dissolved in a small amount of 10 mM Tris–HCl buffer, pH 7.8, and dialyzed against the same buffer (5-liter) for 2 d. After centrifugation, the resulting supernatant (total $OD_{280\,nm}$, $A_{280\,nm}$ × sample volume = 717.60) was applied to a DEAE cellulose column (4 × 40 cm) equilibrated with 10 mM Tris–HCl buffer, pH 7.8. The run-through fraction was pooled and dialyzed against 10-liter (5-liter × 2 times) of 10 mM Na-acetate buffer, pH 5.0, containing 0.1 M NaCl for 2 d. The dialyzate was applied to a SP-Toyopearl (3 × 22 cm) column equilibrated with the same buffer. After the column was washed with the same buffer (about 600 ml), bound proteins were eluted by 10 mM Na-acetate buffer, pH 5.0, containing 0.5 M NaCl. The bound fraction (the Cha o 1 fraction) was dialyzed against 10-liter (5-liter × 2 times) of 10 mM Na-acetate buffer, pH 5.0, containing 0.1 M NaCl for 2 d, and the resulting dialysate (total $OD_{280\,nm}$ = 29.68) was applied to the SP-Toyopearl (3 × 22 cm) column equilibrated with the same buffer. In a second cation-exchange chromatography, the bound proteins were eluted by a linear gradient of NaCl from 0.1 M to 0.5 M in 10 mM Na-acetate buffer, pH 5.0. The Cha o 1 fraction, indicated by a horizontal bar in Fig. 1-A, was pooled and concentrated to about 7 ml by Amicon Centriprep-30. The total $OD_{280\,nm}$ of the concentrated sample was 5.26. Cha o1 was further purified by gel-filtration with a Superdex 200 column (GE-Healthcare, 1.6 × 120 cm) in 25 mM Tris–HCl buffer, pH 7.8, containing 0.1 M NaCl. As shown in Fig. 1-B, Cha o 1 was separated from some other contaminative proteins, but two protein bands (around 47 kDa) were detected on the SDS-gel by CBB staining (Fig. 2-I) and on the PVDF membrane by immunoblotting using the antiserum against Cha o 1 (Fig. 2-II), suggesting that Cha o 1 occurs in several isoforms, as reported by Suzuki *et al.*[4] Furthermore, as shown in Fig. 2-III, the purified Cha o 1 was recognized by the

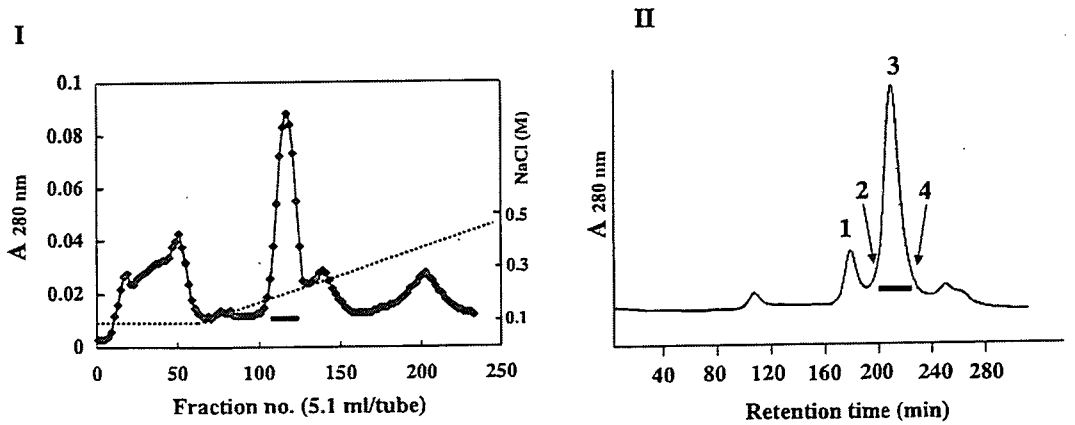

Fig. 1. Purification of Cha o 1.

I, SP-Toyopearl chromatography of partially purified Cha o1. Partially purified Cha o 1 was loaded on a SP-Toyopearl column in 10 mM Na-acetate buffer, pH 5.0. The allergen was eluted by a linear gradient of NaCl from 0.1 M to 0.5 M in 10 mM Na-acetate buffer, pH 5.0. The Cha o 1-containing fraction, detected by immunoblotting, was pooled as indicated by a horizontal bar. II, Gel-filtration of the Cha o 1 fraction obtained in I. The concentrated Cha o 1 fraction obtained by SP-Toyopearl chromatography was loaded on a Superdex 200 column (1.6 × 120 cm). The column was developed with 25 mM Tris–HCl buffer, pH 7.8, containing 0.1 M NaCl at a flow rate of 0.8 ml/min.

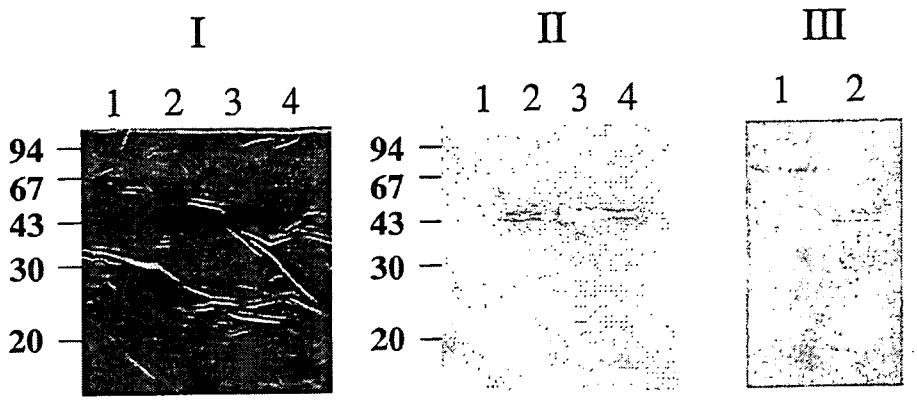

Fig. 2. SDS–PAGE and Immunoblotting.
I, CBB staining of 20% polyacrylaminde gel. Lane 1, peak 1 in Fig. 1-II; lane 2, position 2 in Fig. 1-II; lane 3, peak 3 in Fig. 1-II; lane 4, position 4 in Fig. 1-II. II, Immunoblotting using anti-Cha o 1 antibody. Lane 1, peak 1 in Fig. 1-II; lane 2, position 2 in Fig. 1-II; lane 3, peak 3 in Fig. 1-II; lane 4, position 4 in Fig. 1-II. III, Immunoblotting using anti-β1-2xylose antibody. Lane 1, peak 1 in Fig. 1-II; lane 2, peak 3 in Fig. 1-II. Each immunoblot was done as described in previous papers.[4,8]

anti-β1-2 xylose antibody,[7,8] indicating that Cha o 1 bears plant-complex type *N*-glycans. After two protein bands were cut on PVDF membrane separately, each N-terminal amino acid sequence was analyzed, and it was found that the two proteins had the same N-terminal sequence (D-N-P-I-D-), indicating that they were Cha o 1. Based on these results, we used the Cha o 1 fraction, indicated by a horizontal bar in Fig. 1-II, in glycoform analysis without further purification.

Preparation of pyridylaminated N-glycans from Cha o 1. *N*-Glycans were released by hydrazinolysis (100 °C, 12 h, in 200 µl of anhydrous hydrazine) from the lyophilized Cha o 1 (2.6 mg). After *N*-acetylation of the hydrazinolysate with saturated ammonium bicarbonate (400 µl) and acetic anhydride (20 µl), the acetylated hydrazinolysate was desalted using Dowex 50 × 2 resins. Pyridylamination of the sugar chains was done by the method of Natsuka and Hase.[9] Separation of PA-sugar chains was done by HPLC on a Jasco 880-PU HPLC apparatus with a Jasco 821-FP Intelligent Spectrofluorometer, using the Shodex Asahipak NH2P-50 column (0.46 × 25 cm) and the Cosmosil 5C18-AR column (0.6 × 25 cm). On the Cosmosil 5C18-AR column, the PA-sugar chains were eluted by increasing the acetonitrile concentration in 0.05% TFA linearly from 0 to 10% at a flow rate 1.2 ml/min. In the case of size-fractionation HPLC using the Asahipak NH2P-50 column, the PA-sugar chains were eluted by increasing the water content in the water-acetonitrile mixture from 36% to 62% linearly for 60 min at a flow rate of 0.7 ml/min.

Electrospray ionization (ESI) mass spectrometry. ESI-MS analysis of PA-sugar chains was done as described in our previous reports,[5,6] using a Perkin Elmer Sciex API-III triple-quadrupole mass spectrometer with an atmospheric-pressure ionization ion source.

Glycosidase digestion of PA-sugar chains. Digestion with jack bean α-mannosidase, diplococcal β-*N*-acetylglucosaminidase, and *Aspergillus* α-1,2-mannosidase was done using about 200 pmol of the PA-sugar chains under the conditions described in our previous reports.[5,10] The resulting glycosidase-digests were analyzed by SF-HPLC using the Asahipak NH2P-50 column (0.46 × 25 cm).

Results and Discussion

Purification of PA-sugar chains

First, the PA-sugar chains from Cha o 1 were partially purified by RP-HPLC, as shown in Fig. 3. Three peaks

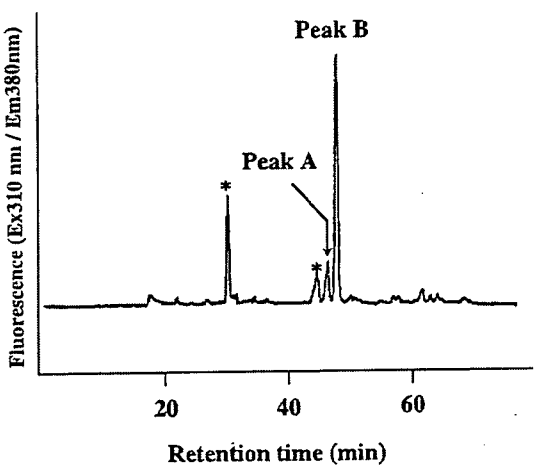

Fig. 3. RP-HPLC Profiles of PA-Sugar Chains from Cha o 1.
Peak A and peak B were confirmed to be relevant N-glycans by ESI-MS, and were used for structural analysis. PA-derivatives were loaded on the Cosmosil 5C 18-AR column (6.0 × 250 mm) equilibrated with 0.05% TFA. The PA-sugar chains were eluted by an increase in acetonitrile concentration. Star mark (*) shows contaminative peaks.

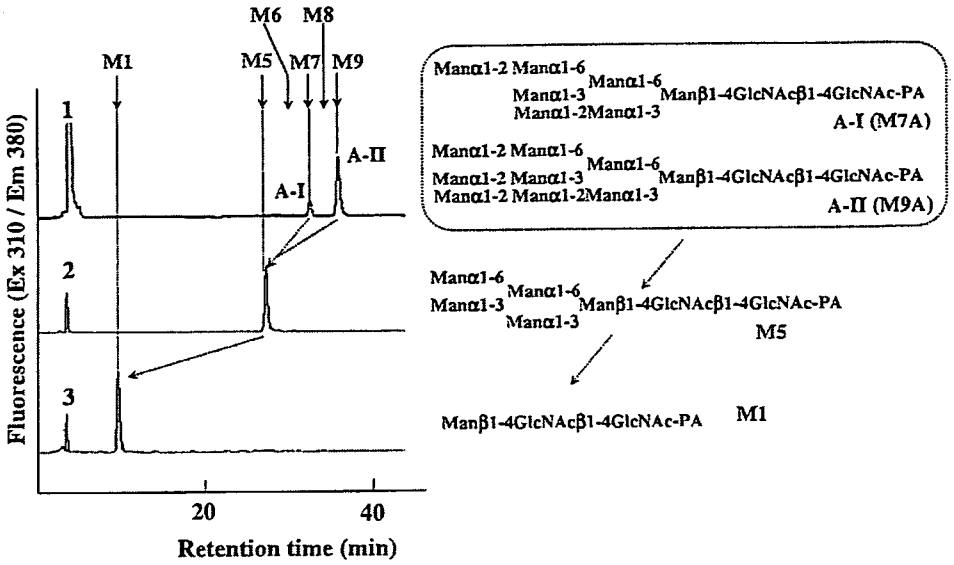

Fig. 4. SF-HPLC of Exoglycosidase Digests of Peak A.

1, PA-sugar chains in peak A in Fig. 3; 2, the *Aspergillus* α-1,2-mannosidase digest of 1; 3, the jack bean α-mannosidase digest of 2. Arrows (M1, M5, M6, M7, M8, and M9) indicate the elution positions of authentic PA-sugar chains: Man1GlcNAc2-PA, Man5GlcNAc2-PA, Man6GlcNAc2-PA, Man7GlcNAc2-PA, Man8GlcNAc2-PA, and Man9GlcNAc2-PA.

were observed in the region where *N*-glycans are expected to be eluted (40–70 min), but it was determined by exoglycosidase digestion that peaks A and B were relevant pyridylaminated *N*-glycans. A small peak eluted just before peak A was not digested by some exoglycosidases, suggesting that this peak might not be *N*-glycan, although MS/MS analysis of it to confirm the presence of GlcNAc-PA (*m/z* 300) could not be done due to the small amount of the sample.

Structures of PA-sugar chains peak A

When peak A in Fig. 3 was analyzed by SF-HPLC, two PA-sugar chains were detected, as shown in Fig. 4-1. The elution positions of these two PA-sugar chains corresponded to those of authentic PA-sugar chains: A-I to Man7GlcNAc2 and A-II to Man9-GlcNAc2-PA. Furthermore, the elution positions of A-I and A-II on RP-HPLC corresponded to those of M7A and M9A respectively. When these PA-sugar chains were treated with *Aspergillus* α-1,2-mannosidase, a new product was eluted at the elution position of M5A (Man5GlcNAc2-PA), suggesting that A-I and A-II contained two and four α1-2 mannose residues respectively (Fig. 4-2). The product was further converted to M1 (Man1GlcNAc2-PA) by jack bean α-mannosidase, as shown in Fig 4-3.

From these results, the structures of A-I and A-II were proposed to be M7A and M9A, respectively, as shown in Fig. 4.

Structural analysis of N-glycans in peak B

As shown in Fig. 5-I, only one PA-sugar chain was detected in peak B in Fig. 3. The elution position corresponded to that of GN2M3FX. The elution position of this PA-sugar chain on RP-HPLC also corresponded to that of GN2M3FX (data not shown), suggesting that the structure of this *N*-glycan is the biantennary plant complex type structure, GlcNAc2Man3Xyl1Fuc1GlcNAc2. ESI-MS analysis of peak B showed a single signal at *m/z* 1674.5 $[(M+H)^+]$ (Fig. 5-II), suggesting that this PA-sugar chain consisted of (HexNAc)3(Hex)3(Deoxyhex)1(Pen)1(HexNAc-PA) or GlcNAc2-Man3Xyl1Fuc1GlcNAc2-PA. The deduced structure was further confirmed by exoglycosidase digestion. This PA-sugar chain was converted to M3FX with diplococcal β-*N*-acetylglucosaminidase, suggesting that two GlcNAc residues were bound by a β1-2 linkage (Fig. 5-I-2). The product was further converted to MFX by jack bean α-mannosidase digestion (Fig. 5-I-3). The data of 2-D sugar chain mapping, exoglycosidase digestion, and ESI-MS analysis suggested that the structure of peak B was GN2M3FX, as shown in Fig. 5.

Comparison of *structural feature of N-glycans linked to cedar pollen allergen (Jun a 1 and Cry j 1) and cypress pollen allergen (Cha o 1)*

As shown in Table 1, we have found that the cedar pollen allergens (Jun a 1 and Cry j 1) carry plant-complex type *N*-glycans containing the Lewis a antigen (Galβ1-3(Fucα1-4)GlcNAcβ1-) unit.[1,2] In addition to these two cedar pollen allergens, it has been reported that Arizona cypress pollen allergen, Cup a 1, also bears the Lewis a unit in the *N*-glycan moiety.[3] Although the physiological function of the Lewis a unit in plant *N*-glycans is still obscure, there is a possibility that the antigenic unit is involved in the symptoms of pollinosis.

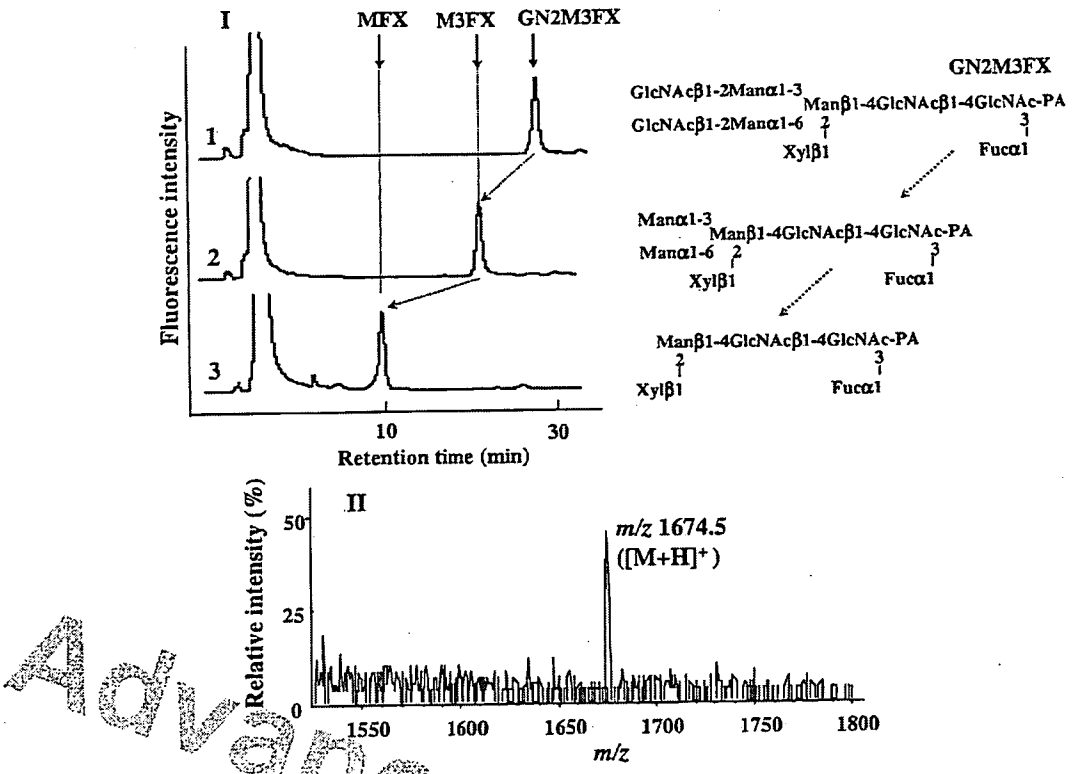

Fig. 5. SF-HPLC of Exoglycosidase Digests of Peak B and ESI-MS Spectrum.
I, SF-HPLC of exoglycosidase digests of peak B. 1, PA-Sugar chain in peak B in Fig. 3; 2, the diplococcal β-GlcNAc-ase digest of I; 3, the jack bean α-mannosidase digest of 2. II, ESI-MS spectrum of Peak B. The PA-sugar chain was observed as a single charged ion, $[M+H]^+$.

Table 1. Comparison of *N*-Glycan Structures of Two Cedar Pollen Allergens (Jun a 1, Cry j 1) and Cha o 1

Structures of *N*-Glycans	Jun a 1-A[a]	Jun a 1-B[a]	Cry j 1[b]	Cha o 1
GlcNAcβ1-2 {Manα1-6, Manα1-3} Manβ1-4GlcNAcβ1-4GlcNAc; Xyl β1 (2); Fuc α1 (3)	ND	3%	ND	ND
GlcNAcβ1-2Man α1-6, GlcNAcβ1-2Man α1-3 Manβ1-4GlcNAcβ1-4GlcNAc; Xyl β1 (2); Fuc α1 (3); Fucα1 (4)	75%	76%	47%	89%
Galβ1-3GlcNAcβ1-2 Man α1-6, Man α1-3 Man β1-4GlcNAc β1-4GlcNAc; Xyl β1 (2); Fuc α1 (3); Fucα1 (4)	23%	21%	38%	ND
Galβ1-3GlcNAcβ1-2 Man α1-6, Galβ1-3GlcNAcβ1-2 Man α1-3 Man β1-4GlcNAc β1-4GlcNAc; Xyl β1 (2); Fuc α1 (3); Fucα1 (4)	2%	ND	15%	ND
Manα1-2Manα1-6, Manα1-2Manα1-3, Manα1-2Manα1-2Manα1-3 Manβ1-4GlcNAcβ1-4GlcNAc	ND	ND	ND	9%
Manα1-2Manα1-6, Manα1-3, Manα1-2Manα1-3 Manβ1-4GlcNAcβ1-4GlcNAc	ND	ND	ND	2%

a, reference 1; b, reference 2

Hence, in this study, we analyzed the glycoform of *N*-glycans of Japanese cypress pollen allergen, Cha o 1, one of the major pollen glycoallergens in Japan. Molecular cloning of Cha o 1 revealed that this Japanese cypress pollen allergen is highly homologous with the two cedar pollen allergens (Cry j 1 and Jun a 1), and that there are six Asn-X-Thr/Ser sequences.[4] Although two (Asn(259)-Pro-Thr(261) and Asn(272)-Asp-Thr(274)) of them might not be glycosylated, it is not known whether the remaining four *N*-glycosylation sites are actually glycosylated. As described in a previous report,[4] Cha o 1 was purified in two isoforms with the same *N*-terminal amino acid sequence (D-N-D-I-P) but different molecular weights (Fig. 2-I), and these two isoforms were recognized by the antiserum against plant complex type *N*-glycans (Fig. 2-III). The difference in molecular weight of the two Cha o 1 molecules might reflect the difference in the numbers of actually glycosylated sites in the four *N*-glycosylation consensus sequences.

Structural analysis of *N*-glycans revealed that the complex type *N*-glycan harboring the Lewis a epitope did not occur in Cha o 1 and that major structure was the biantenary plant complex type structure: GlcNAc-β1-2Manα1-6(GlcNAcβ1-2Manα1-3)(Xylβ1-2)Manβ1-4GlcNAcβ1-4 (Fucα1-3)GlcNAc (GN2M3FX) (Fig. 5 and Table 1). This result suggest that the Lewis a epitope in the *N*-glycan moiety is not involved in the symptoms of pollinosis. It is noteworthy, however, that a high content of the GM2M3FX structure is a common feature of the *N*-glycans of allergenic pollen glycoproteins (Jun a 1, Cry j 1, Cup a 1, olive pollen allergen Ole e1, *Ginkgo biloba* pollen glycoprotein, and palm pollen glycoprotein).[1–3,11–13] Comparing the cedar pollen allergens (Jun a 1 and Cry j 1) and Arizona cypress pollen allergens (Cup a 1), the occurrence of high-mannose type *N*-glycans appears to be specific to Japanese cypress pollen allergen (Cha o 1), although the content is very low. Among plant glycoallergens, it has been reported that a peanut allergen, Ara h 1, carries the high-mannose type *N*-glycans (Man6-5GlcNAc2) in addition to xylosylated *N*-glycans.[11] And recently it has been proposed that the *N*-glycan of Ara h 1 is a ligand of dendritic cell-specific ICAM-grabbing nonintegrin (DC-SIGN) and that it acts as a Th2 ajuvant.[14] Since DC-SIGN is a C-type lectin specific to mannose residues in glycans, it is possible to assume that the *N*-glycans linked to Cha o 1 are ligands of DC-SIGN, and that Cha o 1 can prime Th2-skewed T-cell responses. Detail analysis of the immunological activity of the *N*-glycans of Cha o1 to dendritic cells is necessary to determine the involvement of plant *N*-glycans in the symptoms of pollinosis.

Acknowledgments

This work was supported in part by grants from the Ministry of Education, Culture, Sports, Science, and Technology of Japan (Basic Research (C), no. 17580300) and the Okayama University COE program, Establishment of Plant Health Science. The authors are grateful to the ESI-MS Laboratory of Okayama University.

References

1) Kimura, Y., Kamamoto, M., Maeda, M., Okano, M., Yokoyama, M., and Kino, K., Occurrence of Lewis a epitope in N-glycans of a glycoallergen, *Jun a 1*, from mountain cedar pollen. *Biosci. Biotechnol. Biochem.*, **69**, 137–144 (2005).
2) Maeda, M., Kamamoto, M., Yamamoto, S., Kimura, M., Okano, M., and Kimura, Y., Glycoform analysis of Japanese cedar pollen allergen, Cry j1. *Biosci. Biotechnol. Biochem.*, **69**, 1700–1705 (2005).
3) Alisi, C., Afferni, C., Iacovacci, P., Barletta, B., Tinghino, R., Butteroni, C., Puggioni, E. M. R., Wilson, I. B. H., Federico, R., Schinina, M. E., Ariano, R., Di Felice, G., and Pini, C., Rapid isolation, charcterization, and glycan analysis of Cup a 1, the major allergen of Arizona cypress (*Cupressus arizonica*) pollen. *Allergy*, **56**, 978–984 (2001).
4) Suzuki, M., Komiyama, N., Itoh, M., Itoh, H., Sone, T., Kino, K., Takagi, I., and Ohta, N., Purification, characterization and molecular cloning of Cha o 1, major allergen of *Chamaecyparis obtuse* (Japanese cypress) pollen. *Mol. Immunol.*, **33**, 451–460 (1996).
5) Maeda, M., and Kimura, Y., Glycoform analysis of *N*-glycans linked to glycoproteins expressed in rice culture cells: predominant occurrence of complex type *N*-glycans. *Biosci. Biotechnol. Biochem.*, **70**, 1356–1363 (2006).
6) Kimura, Y., Miyagi, C., Kimura, M., Nitoda, T., Kawai, N., and Sugimoto, H., Structural features of *N*-glycans linked to royal jelly glycoproteins. *Biosci. Biotechnol. Biochem.*, **64**, 2109–2120 (2000).
7) Kimura, Y., Hess, D., and Strum, A., The *N*-glycans of jack bean α-mannosidase: structure, topology, and function. *Eur. J. Biochem.*, **264**, 168–175 (1999).
8) Kimura, Y., Harada, T., Matsuo, S., and Yonekura, M., Purification and some chemical properties of 30 kDa *Ginkgo biloba* glycoprotein, which reacts with antiserum against β1→2 xylose-containing N-glycans. *Biosci. Biotechnol. Biochem.*, **63**, 163–167 (1999).
9) Natsuka, S., and Hase, S., Analysis of *N*- and *O*-glycans by pyridylamination. *Methods Mol. Biol.*, **76**, 101–113 (1998).
10) Kato, T., Kitamura, K., Maeda, M., Kimura, Y., Katayama, T., Ashida, H., and Yamamoto, K., Free oligosaccharides in the cytosol of *Caenorhabditis elegance* are generated through endoplasmic reticulum-Golgi trafficking. *J. Biol. Chem.*, **282**, 22080–22088 (2007).
11) Kolarich, D., and Altmann, F., N-Glycan analysis by matrix-assisted laser desorption/ionization mass spectrometry of electrophoretically separated nonmammalian proteins: application to peanut allergen Ara h 1 and olive pollen allergen Ole e 1. *Anal. Biochem.*, **285**, 64–75 (2000).
12) Kimura, Y., Suzuki, M., and Kimura, M., *N*-Linked oligosaccharides of glycoproteins from allergenic

Ginkgo biloba pollen. *Biosci. Biotechnol. Biochem.*, **65**, 2001–2006 (2001).

13) Kimura, Y., Yoshiie, T., Woo, K. K., Maeda, M., Kimura, M., and Tan, S. H., Structural features of *N*-glycans linked to glycoproteins from oil palm pollen, an allergenic pollen. *Biosci. Biotechnol. Biochem.*, **67**, 2232–2239 (2003).

14) Shreffler, W. G., Castro, R. R., Kucuk, Z. Y., Charlos-Powers, Z., Grishina, G., Yoo, S., Burks, A. W., and Sampson, H. A., The major glycoprotein allergen from *Arachis hypogaea*, Ara h 1, is a ligand of dendritic cell-specific ICAM-grabbing nonintegrin and acts as a Th2 adjuvant *in vitro*. *J. Immunol.*, **177**, 3677–3685 (2006).

balt6/zim-jimm/zim-jimm/zim00808/zim6937-08z | xppws | S=1 | 2/28/08 | 16:32 | 4/Color Figure(s): F3,6 | Art: 6937 | Input-kco

The Journal of Immunology

CRTH2 Plays an Essential Role in the Pathophysiology of Cry AQ:A,B j 1-Induced Pollinosis in Mice[1]

Rie Nomiya,* Mitsuhiro Okano,* Tazuko Fujiwara,* Megumi Maeda,† Yoshinobu Kimura,† Kosuke Kino,‡ Minehiko Yokoyama,‡ Hiroyuki Hirai,§ Kinya Nagata,§ Toshifumi Hara,¶ Kazunori Nishizaki,* and Masataka Nakamura[2,¶]

PGD_2 is the major prostanoid produced during the acute phase of allergic reactions. Two PGD_2 receptors have been isolated, DP and CRTH2 (chemoattractant receptor-homologous molecule expressed on Th2 cells), but whether they participate in the pathophysiology of allergic diseases remains unclear. We investigated the role of CRTH2 in the initiation of allergic rhinitis in mice. First, we developed a novel murine model of pollinosis, a type of seasonal allergic rhinitis. Additionally, pathophysiological differences in the pollinosis were compared between wild-type and *CRTH2* gene-deficient mice. An effect of treatment with ramatroban, a CRTH2/T-prostanoid receptor dual antagonist, was also determined. Repeated intranasal sensitization with Cry j 1, the major allergen of *Cryptomeria japonica* pollen, in the absence of adjuvants significantly exacerbated nasal hyperresponsive symptoms, Cry j 1-specific IgE and IgG1 production, nasal eosinophilia, and Cry j 1-induced in vitro production of IL-4 and IL-5 by submandibular lymph node cells. Additionally, CRTH2 mRNA in nasal mucosa was significantly elevated in Cry j 1-sensitized mice. Following repeated intranasal sensitization with Cry j 1, *CRTH2* gene-deficient mice had significantly weaker Cry j 1-specific IgE/IgG1 production, nasal eosinophilia, and IL-4 production by submandibular lymph node cells than did wild-type mice. Similar results were found in mice treated with ramatroban. These results suggest that the PGD_2-CRTH2 interaction is elevated following sensitization and plays a proinflammatory role in the pathophysiology of allergic rhinitis, especially pollinosis in mice. *The Journal of Immunology*, 2008, 179: 0000–0000.

Pollinosis, a type of seasonal allergic rhinitis, is the most common allergic respiratory disease and is a global health problem that is increasing in prevalence (1–3). For example, as much as 10–20% of the Japanese population suffers from Japanese cedar pollinosis (JCP)[3](3).

Intensive and extensive studies on pollinosis have greatly improved the understanding of its etiology and pathology (4). Mouse models of allergic rhinitis have contributed to these advances. However, these mouse models usually use adjuvants and/or strong Ags to efficiently sensitize animals (5–9). To further examine the pathophysiological mechanism underlying pollinosis, a murine model that naturally mimics human pollinosis by intranasal administration of pollen extracts in the absence of adjuvants is needed.

Prostanoids are thought to participate in allergic inflammation (10). PGD_2 is one of the most important of these and it plays roles in allergic respiratory diseases including allergic rhinitis (10–15). For example, nebulized PGD_2 enhances Th2-type inflammatory responses and eosinophilia, leading to the development of airway hyperresponsiveness (14). PGD_2 acts via the D-prostanoid receptor (DP) and chemoattractant receptor-homologous molecule expressed on Th2 cells (CRTH2) (16). The expression patterns and signaling pathways utilized by DP and CRTH2 are different, suggesting that they have distinct roles in allergic responses (16, 17). It appears that signals via DP promote eosinophil survival, whereas signals via CRTH2 mediate shape changes, chemotaxis, and degranulation by eosinophils (16, 18, 19).

The role of CRTH2 in allergic airway inflammation in vivo remains controversial (17). CRTH2 has been found to participate in the recruitment of eosinophils from the bone marrow into the bloodstream (19, 20), in eosinophilic airway inflammation (11), and in airway eosinophilia and hyperresponsiveness (21), suggesting that it plays a proinflammatory role in vivo. On the other hand, mice deficient for CRTH2 ($CRTH2^{-/-}$) show eosinophil recruitment and IL-5 production by splenocytes in an asthma model, suggesting that CRTH2 mediates antiinflammatory signals (22). In human nasal mucosa, CRTH2 is expressed in eosinophils and a subset of T cells (23). We have recently reported that there is a close correlation between the number of eosinophils infiltrating into nasal mucosa and the amount of CRTH2, but not DP, in nasal mucosa (12). Also, $CRTH2^{-/-}$ mice have been found to show reduced eosinophil infiltration into skin in a model of chronic allergic skin inflammation (24).

In this study, we established a novel murine model of pollinosis and used it to determine the pathophysiological role of CRTH2 in

*Department of Otolaryngology–Head and Neck Surgery, Okayama University Graduate School of Medicine, Dentistry and Pharmaceutical Sciences, Okayama, Japan; †Division of Biomolecular Science, The Graduate School of Natural Science and Technology, Okayama University, Okayama, Japan; ‡Meiji Co., Odawara, Japan; §Department of Advanced Medicine and Development, BioMedical Laboratories, Inc., Saitama, Japan; and ¶Human Gene Sciences Center, Tokyo Medical and Dental University, Tokyo, Japan

Received for publication July 23, 2007. Accepted for publication February 8, 2008.

The costs of publication of this article were defrayed in part by the payment of page charges. This article must therefore be hereby marked *advertisement* in accordance with 18 U.S.C. Section 1734 solely to indicate this fact.

[1] This work was supported in part by grants from the Ministry of Education, Culture, Sports, Science, and Technology, Japan (14704143), and Research on Allergic Disease and Immunology of the Ministry of Health, Labor, and Welfare, Japan (14210301).

AQ: F [2] Address correspondence and reprint requests to Dr. Mitsuhiro Okano, Okayama Graduate School of Medicine, Dentistry, and Pharmaceutical Sciences, 2-5-1 Shikata-cho, 700-8558 Okayama, Japan. E-mail address: mokano@cc.okayama-u.ac.jp

AQ: G [3] Abbreviations used in this paper: JCP, Japanese cedar pollinosis; CRTH2, chemoattractant receptor-homologous molecule expressed on Th2 cells; DP, D-protanoid receptor; TP, T-prostanoid receptor; WT, wild type.

balt6/zim-jimm/zim-jimm/zim00808/zim6937-08z | xppws | S=1 | 2/28/08 | 16:32 | 4/Color Figure(s): F3,6 | Art: 6937 | Input-kco

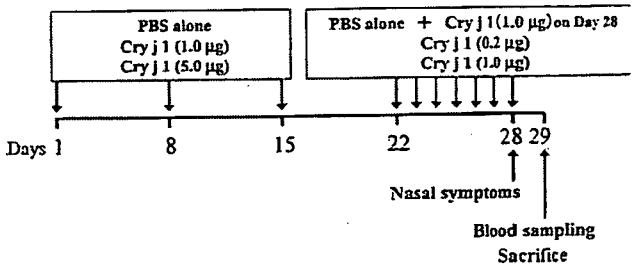

FIGURE 1. Experimental design used to investigate the effect of nasal exposure to Cry j 1 in mice. BALB/c mice (6–9 per group) were sensitized by intranasal administration of either 1.0 or 5.0 μg of Cry j 1 in 10 μl PBS in the absence of adjuvants once a week for 3 wk (on days 1, 8, and 15). One week after the third sensitization, mice were challenged by intranasal administration of 0.2 or 1.0 μg of Cry j 1, respectively every day for 7 consecutive days (on days 22 to 27). As a control, mice were treated with PBS, except for the final challenge, where mice were treated with 1.0 μg of Cry j 1. Immediately after the final nasal challenge, nasal symptoms were observed for 10 min, and 16 h after the final nasal challenge, peripheral blood was collected, and the specific Ab content in the serum was measured. After the blood sampling, mice were sacrificed, and the nose and submandibular lymph nodes were obtained for further analysis.

the disease. In this model, intranasal sensitization with Cry j 1, the major allergen of *Cryptomeria japonica* pollen, in the absence of adjuvant induced allergic rhinitis closely resembling human pollinosis. We found that a lack of CRTH2 in the mutant mice greatly reduces allergic pathophysiologies in this model.

Materials and Methods

Animals and Ags

BALB/c mice were purchased from Charles River Laboratories Japan and CLEA Japan. Homozygous CRTH2-deficient and wild-type BALB/c mice were obtained as described previously (24). Female mice (7–11 wk old) were used in all the experiments. The mice were maintained in specific pathogen-free conditions at Okayama University and Tokyo Medical and Dental University in accordance with the guidelines set forth by the university committees. All experimental protocols and procedures in the present study were approved by the University Animal Care and Use Committees. Cry j 1 was purified from crude extracts of *C. japonica* pollen as described previously (25). Endotoxin contamination was considered to be negligible due to a negative result in the Endospec ES test (Seikagaku). Ramatroban was obtained from Bayer Yakuhin. Protein concentrations were determined using a bicinchoninic acid assay (Pierce) according to the manufacturer's instructions.

Sensitization of mice

Mice (6–9 animals per group) were sensitized by intranasal application of serial doses of Cry j 1 in 10 μl PBS in the absence of adjuvants using a microsyringe (Hamilton Medical). The low-dose sensitization consisted of a series of administrations of 1.0 μg of Ag once a week for 3 wk (on days 1, 8, and 15), followed by administration of 0.2 μg Ag every day for 7 consecutive days (on days 22 to 28). For high-dose sensitization, 5.0 and 1.0 μg of Cry j 1 were administered once a week for 3 wk (on days 1, 8, and 15) and every day for 7 consecutive days (on days 22 to 28), respectively. As a control, mice were treated with PBS instead of the Ag at all points except for the final challenge, where the mice were administered 1.0 μg of Cry j 1 (Fig. 1). Immediately after the final nasal challenge, the frequencies of sneezing and nasal rubbing were counted in a blinded manner for 10 min. Peripheral blood was collected from the tail vein 16 h after the final nasal challenge, and then sera were prepared by centrifugation at 200 × *g*, and the levels of Cry j 1-specific Ab in the serum were determined by ELISA. The mice were then sacrificed, and the nose and submandibular lymph nodes were isolated for further immunological and histological analyses.

To determine whether the effect of CRTH2 deficiency is at the level of sensitization or amplification of allergic cascade, outcomes of pollinosis were compared with CRTH2$^{-/-}$ mice sensitized and subsequently challenged with Cry j 1 and nonsensitized CRTH2$^{-/-}$ mice with a single challenge with Cry j 1.

Ramatroban treatment

Ramatroban was suspended in 5% methyl cellulose and administered orally at a dose of 30 mg/kg body weight once a day from 1 day before the first sensitization to the final challenge (day 0 to day 28). Control mice were given 5% methyl cellulose alone.

Ab determination

The levels of Cry j 1-specific IgE, IgG1, and IgG2a were determined by ELISA as previously described (26). The levels of Cry j 1-specific IgE were measured using biotinylated Cry j 1 (Hayashibara Biochemical Laboratories) as a detecting reagent. The titers of Ag-specific Abs were estimated according to the mean OD at 450 nm of serum dilutions of 1/20 for IgE and 1/100 for IgG1 and IgG2a.

In vitro culture of submandibular lymph node cells and measurement of cytokine production

Submandibular lymph nodules from mice were dispersed and filtered through a 70-μm cell strainer (BD Biosciences) to yield a single-cell suspension. Lymph node cells were suspended in RPMI 1640 supplemented with 10% heat-inactivated FCS (Invitrogen), 100 μg/ml streptomycin, 100 U/ml penicillin, and 20 mM L-glutamine (Sigma-Aldrich). Cells (4×10^5 cells/200 μl) were cultured in the presence or absence of 10 μg/ml Cry j 1 in 96-well flat-bottom plates (BD Biosciences) at 37°C in humidified atmosphere of 5% CO_2 and 95% air. After 72 h of culture, supernatants were harvested. The levels of IL-4, IL-5, and IFN-γ in the culture supernatant were measured using OptEIA sets (BD Biosciences). The levels of IL-13 were measured using DuoSet ELISA development kit (R&D Systems). The detection limits for IL-4, IL-5, IL-13, and IFN-γ in this system were 10, 30, 40, and 60 pg/ml, respectively.

Histological examination

Histological examination was performed as previously described (26). Coronal nasal sections were stained with H&E and Luna solution to detect mononuclear cells and eosinophils, respectively. A blind test was conducted to determine the numbers of infiltrating cells in the posterior part of nasal septum using a high-power (10 × 40) microscopic field.

To determine the infiltration of T cells into nasal mucosa, immunohistochemistry for CD3 was examined. Paraffin-embedded nasal tissues were sectioned into 5-μm slices, deparaffinized, rehydrated and retrieved with microwave. Endogenous peroxidase activity was quenched with 3% H_2O_2, and nonspecific protein binding was blocked with normal rabbit serum (DAKO Japan) for 60 min. After this, the tissue sections were incubated with goat anti-mouse CD3-ε polyclonal Ab (sc-1127: Santa Cruz Biotechnology) or control goat IgG Ab (M-20: Santa Cruz Biotechnology) overnight at 4°C. To detect the reaction, N-Histofine Simple Stain MAX PO (G) (Nichirei Biosciences) and diaminobenzidine substrate (DAKO Japan) was used according to the manufacturers' instructions.

Real-time quantitative PCR in nasal mucosa

Mucosal tissues were removed from nasal septum 16 h following the final nasal challenge, immediately soaked in buffer containing guanidine isothiocyanate from the RNeasy Mini Kit (Qiagen), and stored at −80°C until use. Extraction of total cellular RNA, reverse transcription to generate cDNA, and real-time quantitative PCR were performed using a Chromo4 Real-Time PCR detector (Bio-Rad Laboratories, Hercules) and QuantiTect SYBR Green PCR reagents (Qiagen) as described previously (12). The primer sequences for CRTH2 and GAPDH are shown in Table I. Standard curves for both CRTH2 and GAPDH were generated using a PCR fragment of CRTH2 and plasmid DNA of GAPDH as a standard, respectively. Then absolute copy number of CRTH2 and GAPDH for each sample was calculated, and samples were reported with a CRTH2 copy number relative to GAPDH.

Relative amounts of IL-4, IL-5, IL-13, IFN-γ, IL-1β, IL-6, TNF-α, RANTES, and eotaxin mRNA in nasal mucosa were also measured. The primers used are listed in Table I.

Statistical analysis

Statistical significance was determined by nonparametrical Mann-Whitney *U* tests. *p* values of <0.05 were considered to indicate statistical significance. Values are shown as means ± SEM.

Table I. *Primary sequences used for real-time PCR amplifications*

	Forward Primer	Reverse Primer	Amplification Size (bp)	Genbank Accession No.
IL-4	CCTCACAGCAACGAAGAACA	CTGCAGCTCCATGAGAACAC	133	NM_021283
IL-5	TCAGCTGTGTCTGGGCCACT	TTATGAGTAGGGACAGGAAGCCTCA	133	NM_010558
IL-13	TGCTTGCCTTGGTGGTCTC	CAGGTCCACACTCCATACC	151	NM_008355
IFN-γ	GCGTCATTGAATCACACCTG	ACCTGTGGGTTGTTGACCTC	103	NM_008337
IL-1β	TCCAGGATGAGGACATGAGCAC	GAACGTCACACCAGCAGGTTA	105	NM_008361
IL-6	CCACTTCACAAGTCGGAGGCTTA	GCAAGTGCATCATCGTTGTTCATAC	112	NM_031168
TNF-α	ATGAGCACAGAAAGCATGATC	TCCACTTGGTGGTTTGCTACG	305	NM_013693
RANTES	AGATCTCTGCAGCTGCCCTCA	GGAGCACTTGCTGCTGGTGTAG	170	NM_013653
Eotaxin	CAGATGCACCCTGAAAGCCATA	TGCTTTGTGGCATCCTGGAC	96	NM_011330
CRTH2	TCTCAACCAATCAGCACACC	CCTCCAAGAGTGGACAGAGC	173	NM_009962
GAPDH	ACCACAGTCCATGCCATCAC	TCCACCACCCTGTTGCTGTA	452	NM_008084

Results

Induction of nasal symptoms in Cry j 1-sensitized mice

We first attempted to generate a mouse model mimicking human allergic rhinitis, especially pollinosis, which causes symptoms of nasal symptoms, including sneezing and nasal rubbing, by intranasal administration of Cry j 1. We found a significant and dose-dependent increase in the frequency of sneezing in BALB/c mice sensitized with Cry j 1. Mice that were treated with PBS alone sneezed 1.8 ± 0.3 (mean ± SEM) times in the 10 min following the final Ag administration, whereas they sneezed 5.8 ± 1.2 times and 15.7 ± 2.7 times when treated with low and high doses of Ag, F2 respectively (Fig. 2*A*). Similarly, immediately after the final Ag challenge, nasal rubbing was observed more frequently in mice sensitized with a high dose of Cry j 1 than in control mice (37.3 ± 5.8 vs 11.2 ± 2.7 times in 10 min). At a low dose of Cry j 1, there was no significant increase in the frequency of nasal rubbing (Fig. 2*B*).

Development of Th2-type immune responses in Cry j 1-sensitized mice

To further characterize the pathogenesis of immune responses caused by Cry j 1, we monitored several parameters associated with pollinosis. Nasal challenge with a low or high dose of Cry j 1 caused a considerable increase in the concentration of Cry j 1-specific IgE in sera when measured 1 day after the final challenge (Fig. 2*C*). There was also a significant elevation in the concentration of Cry j 1-specific IgG1 (Fig. 2*D*). The concentration of Cry j 1-specific IgE and IgG1 was not appreciably different at the low and high doses of Cry j 1. Cry j 1, however, had little effect on the level of Cry j 1-specific IgG2a (Fig. 2*E*).

Eosinophil infiltration into nasal mucosa, another characteristic of pollinosis, is rarely seen in the nasal mucosa in control mice (Fig. 3*A*). On the contrary, there was a marked accumulation of F3 eosinophils not only in the lamina propria but also in the epithelial layer in mice 1 day after the final challenge (Fig. 3, *B* and *C*). Eosinophil numbers per field following intranasal Cry j 1 sensitization/challenge at both low and high doses were significantly higher than in control mice (Fig. 3*D*). The nasal mucosa of Cry j 1-sensitized mice also showed severe infiltration by mononuclear cells. The nasal septum of mice treated with low and high doses of Cry j 1 contained more mononuclear cells per field (59.8 ± 9.0 ($p = 0.055$) and 80.2 ± 9.1 ($p = 0.016$), respectively) than did control mice (39.8 ± 4.7).

We next examined the in vitro production of cytokines in culture by cells isolated from submandibular lymph nodes from mice treated in vivo with or without Cry j 1. The amounts of IL-4 and

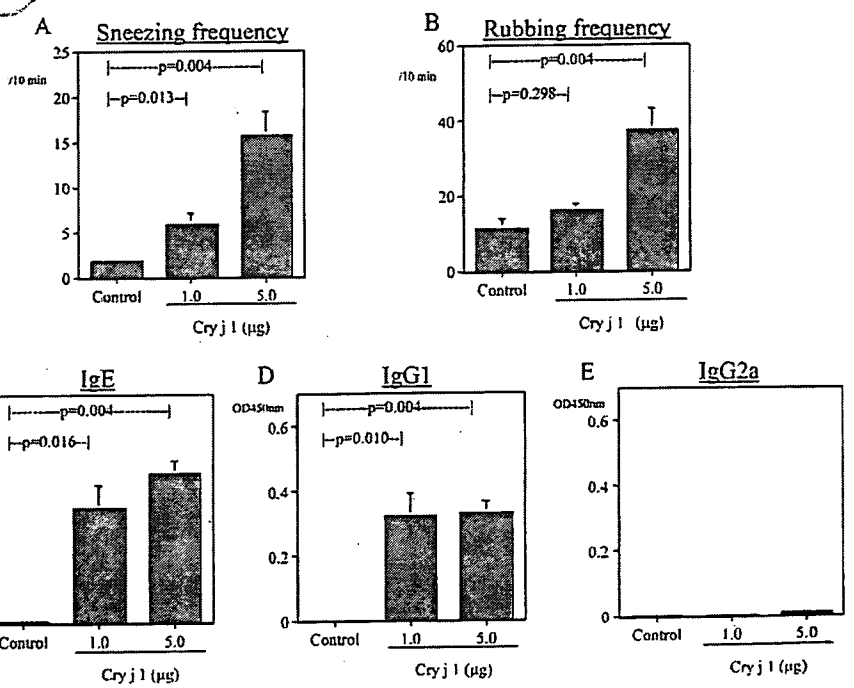

FIGURE 2. Nasal hyperresponsive symptoms and Ab production in mice following intranasal sensitization and challenge with Cry j 1. Mice were sensitized and challenged by intranasal administration of Cry j 1. Nasal allergic symptoms, including the frequency of sneezing (*A*) and rubbing (*B*), were determined for the 10 min immediately following the final nasal challenge (day 28). Mean frequencies ± SEM are shown. Serum samples were obtained 16 h after the final intranasal challenge. Cry j 1-specific IgE (*C*), IgG1 (*D*), and IgG2a (*E*) levels were determined by ELISA. Mean OD values ± SEM are shown. Results are representative of two independent experiments.

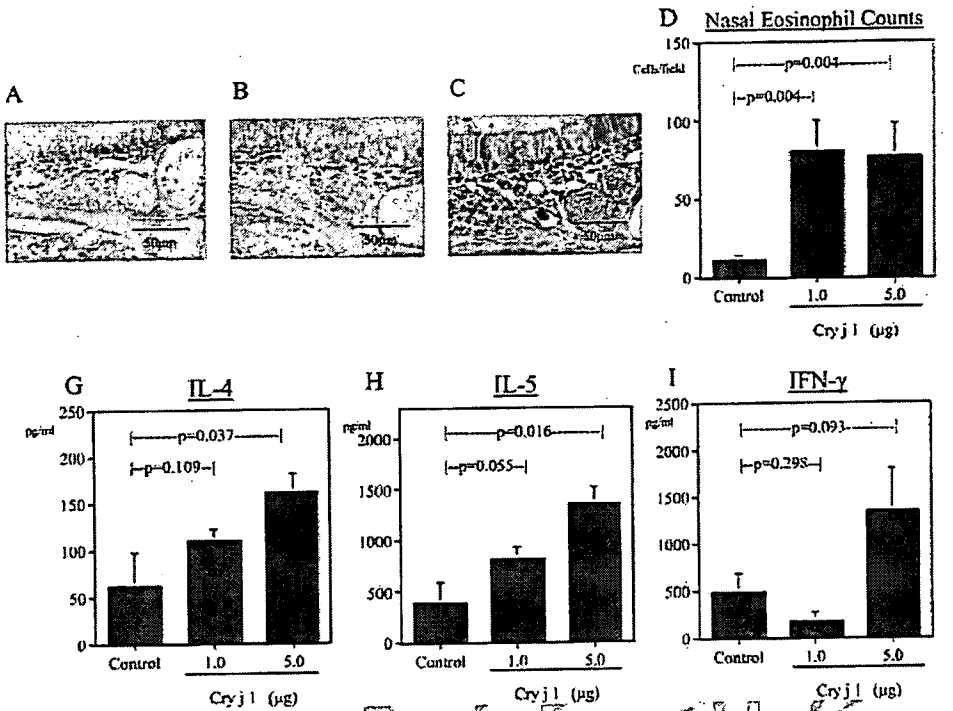

AQ: J **FIGURE 3.** Nasal eosinophilia and cytokine production by submandibular lymph node cells following intranasal sensitization and challenge with Cry j 1. Mice were sensitized and challenged by intranasal administration of PBS (*A*), low-dose Cry j 1 (*B*), or high-dose Cry j 1 (*C*) according to the schedule shown in Fig. 1. Sixteen hours after the final challenge, nasal sections were collected, fixed, and decalcified, and eosinophils in the nasal mucosa were detected by Luna stain. *D*, The numbers of eosinophils in the posterior portion of the nasal septum were determined per high-power (10 × 40) microscopic field. Mean numbers of infiltrating cells per field ± SEM are shown. Sixteen hours after the final challenge, submandibular lymph node cells were isolated and cultured in the absence or presence of Cry j 1 for 72 h. IL-4 (*E*), IL-5 (*F*), and IFN-γ (*G*) were measured by ELISA. Mean concentrations ± SEM are shown. Results are representative of two independent experiments.

IL-5 produced by the cells were in proportion to the doses used for in vivo sensitization (Fig. 3, *E* and *F*). IFN-γ production was slightly enhanced in lymph node cells from mice treated with a high dose of Cry j 1 compared with control mice, but the increase was not statistically significant (Fig. 3*G*).

CRTH2 mRNA expression in nasal mucosa of Cry j 1-sensitized mice

We next measured the expression of CRTH2 at sites of nasal inflammation. Control mice treated with PBS expressed a low level of CRTH2 mRNA in the mucosal tissue of the nasal septum. In mice treated with Cry j 1, the level of CRTH2 mRNA was signif- F4 icantly increased (Fig. 4). Thus, we further investigated whether CRTH2 is positively or negatively involved in the pathophysiology of pollinosis using CRTH2$^{-/-}$ mice.

Impaired pathophysiology of pollinosis in Cry j 1-sensitized CRTH2$^{-/-}$ mice

A high dose of Cry j 1 was administered to both wild-type (WT) and CRTH2$^{-/-}$ mice, and the nasal hyperresponsive symptoms were examined immediately after the final nasal challenge. Notably, the number of sneezes in 10 min by the Cry j 1-sensitized mutant mice was significantly lower than by the WT mice (Fig. F5 5*A*). Nasal rubbing was also significantly lower in the CRTH2$^{-/-}$ mice than in the WT mice (Fig. 5*B*).

The level of Cry j 1-specific IgE in serum samples collected on the day following the final Ag challenge was significantly lower for mutant mice than for WT mice (Fig. 5*C*). Production of Cry j 1-specific IgG1 was similarly reduced in CRTH2$^{-/-}$ mice compared with WT mice (Fig. 5*D*). In contrast, serum levels of Cry j 1-specific IgG2a were the same in the two mouse strains (Fig. 5*E*).

The number of eosinophils infiltrating into the nasal septum following administration of Cry j 1 was also significantly lower in the CRTH2$^{-/-}$ mice than in the WT mice (Fig. 6*A–C*). Although the F6 number of mononuclear cells infiltrating the nasal septum was not significantly different in the mutant and WT mice (Fig. 6*D*), the number of infiltrating CD3$^+$ cells was significantly reduced in CRTH2$^{-/-}$ mice as compared with WT mice (Fig. 6*E*). These

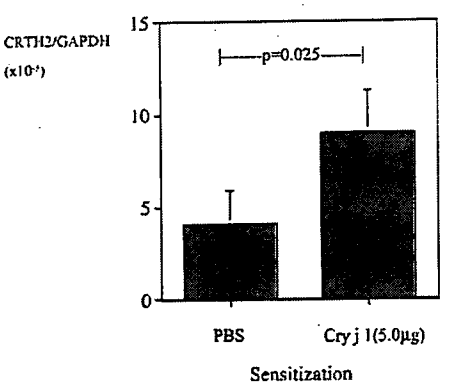

FIGURE 4. Relative amounts of CRTH2 mRNA in nasal mucosa. Mice (6 per group) were sensitized by intranasal administration of 5.0 μg of Cry j 1 once a week for 3 wk. One week after the third sensitization, mice were challenged by intranasal administration of 1.0 μg of Cry j 1 each day for 7 consecutive days. Control animals were treated with PBS at all steps except for the final challenge, where they were treated with 1.0 μg of Cry j 1. Sixteen hours after the final challenge with Cry j 1, mucosal tissues were removed from the nasal septum. The CRTH2 mRNA levels were estimated using real-time quantitative PCR. Results are the mean amounts of mRNA ± SEM.

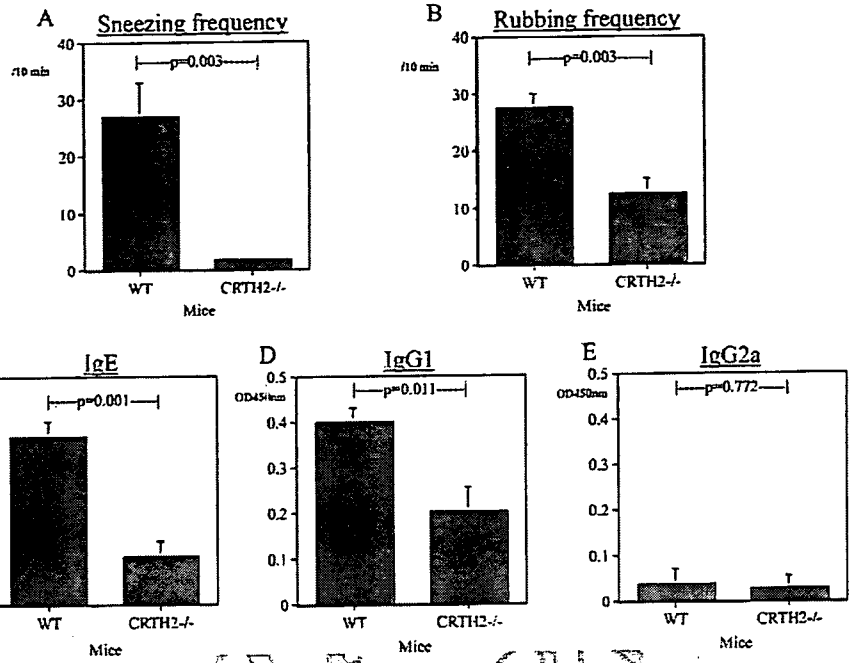

FIGURE 5. Nasal symptoms and Ab production in WT and CRTH2$^{-/-}$ mice following the final nasal challenge with Cry j 1. Mice were sensitized and challenged by intranasal administration of Cry j 1. Sneezing (*A*) and rubbing (*B*) frequency were measured for 10 min following the final nasal challenge (day 28). Mean frequencies ± SEM are shown. Sixteen hours after the final nasal challenge, blood was sampled from mice, and levels of serum Cry j 1-specific IgE (*C*), IgG1 (*D*), and IgG2a (*E*) were determined by ELISA. Mean ODs ± SEM are shown. Results are representative of two independent experiments.

results suggest that CRTH2 deficiency affects infiltration of not only eosinophils but also T cells.

To clarify the link between CRTH2 deficiency and the relief of allergic symptoms, we further investigated cytokine production in vitro by cells from submandibular lymph nodes obtained the day after the final Ag challenge. The amount of IL-4 was 5-fold lower in CRTH2$^{-/-}$ mice than in WT mice (Fig. 6*F*). Additionally, there was a slight reduction in the amount of IL-5 (Fig. 6*G*) and a slight increase in the amount of INF-γ (Fig. 6*I*) in the cells from CRTH2$^{-/-}$ mice, but the differences were not significant. On the contrary, the levels of IL-13 were significantly higher in CRTH2$^{-/-}$ mice as compared with WT mice (Fig. 6*H*).

Additionally, mRNA levels of Th2 cytokines (IL-4, IL-5, and IL-13), Th1 cytokine (IFN-γ), proinflammatory cytokines (IL-1β, IL-6 and TNF-α), and eosinophil-chemotactic chemokines (RANTES and eotaxin) in nasal mucosa were determined. The

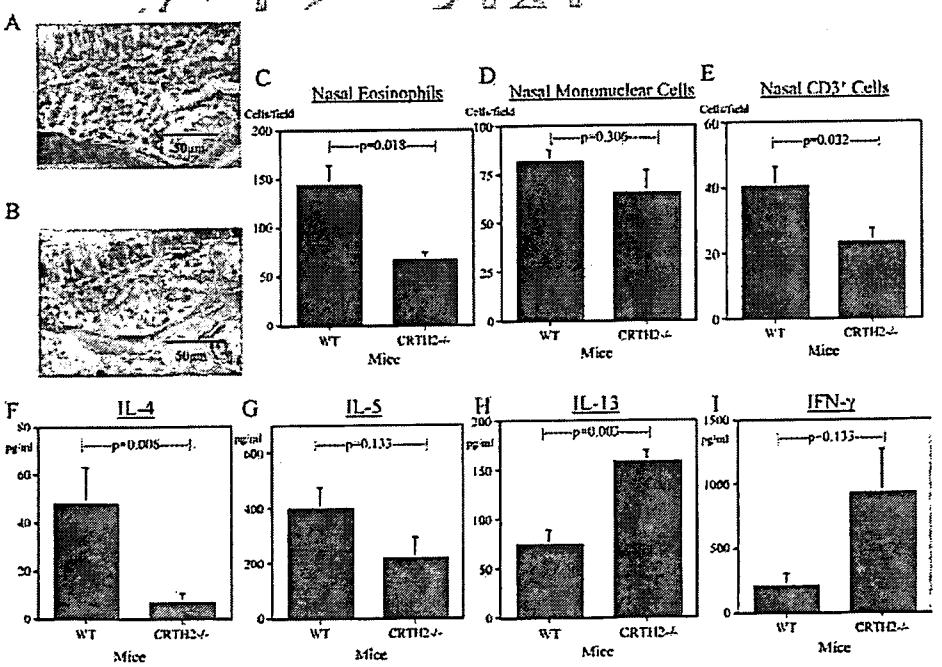

FIGURE 6. Histological changes and cytokine production by submandibular lymphocytes following nasal challenge with Cry j 1 in WT and CRTH2$^{-/-}$ mice. WT (*A*) and CRTH2$^{-/-}$ (*B*) mice were sensitized and challenged by intranasal administration of Cry j 1. Sixteen hours following the final nasal challenge with Cry j 1, nasal sections were collected, fixed, and decalcified, and eosinophils in nasal mucosa were detected by Luna stain. *C*, The number of eosinophils in the posterior portion of the nasal septum was determined per high-power (10 × 40) microscopic field. Mean numbers of infiltrating eosinophils per field ± SEM are shown. Numbers of mononuclear cells (*D*) and CD3$^+$ cell (*E*) in the nasal septum were also determined. Sixteen hours after the final challenge with Cry j 1, submandibular lymph node cells were isolated and cultured with Cry j 1 for 72 h. IL-4 (*F*), IL-5 (*G*), IL-13 (*H*), and IFN-γ (*I*) were measured by ELISA. Mean concentrations ± SEM are shown. Results are representative of two independent experiments.

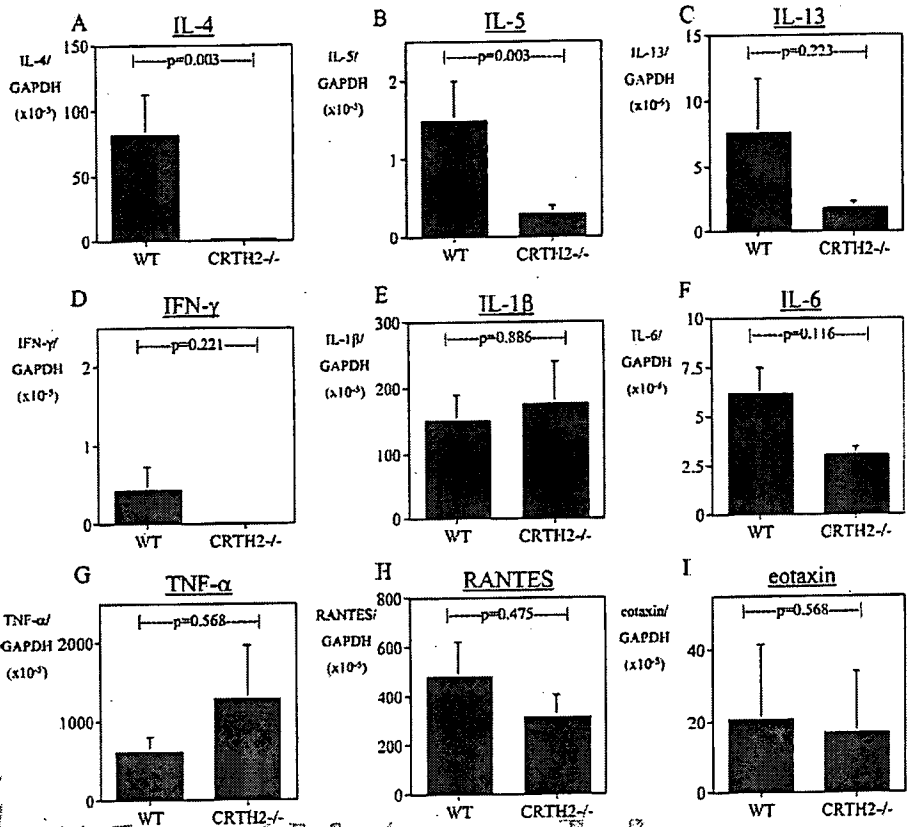

FIGURE 7. Relative amounts of cytokines/chemokines mRNA in nasal mucosa following nasal challenge with Cry j 1 in WT and CRTH2$^{-/-}$ mice. Sixteen hours after the final nasal challenge with Cry j 1, mucosal tissues were removed from nasal septum. Relative amounts of IL-4 (*A*), IL-5 (*B*), IL-13 (*C*), IFN-γ (*D*), IL-1β (*E*), IL-6 (*F*), TNF-α (*G*), RANTES (*H*), and eotaxin (*I*) mRNA were compared between WT and CRTH2$^{-/-}$ mice. Results are the mean amounts of mRNA ± SEM.

levels of IL-4 and IL-5 mRNA were significantly lower in CRTH2$^{-/-}$ mice as compared with WT mice, whereas the levels of other cytokines/chemokines were similar between CRTH$^{-/-}$ and WT mice (Fig. 7). These results suggest that reduced nasal eosinophilia in CRTH2 deficiency is associated with reduced levels of IL-5 but not RANTES or eotaxin in this model. Additionally, F7

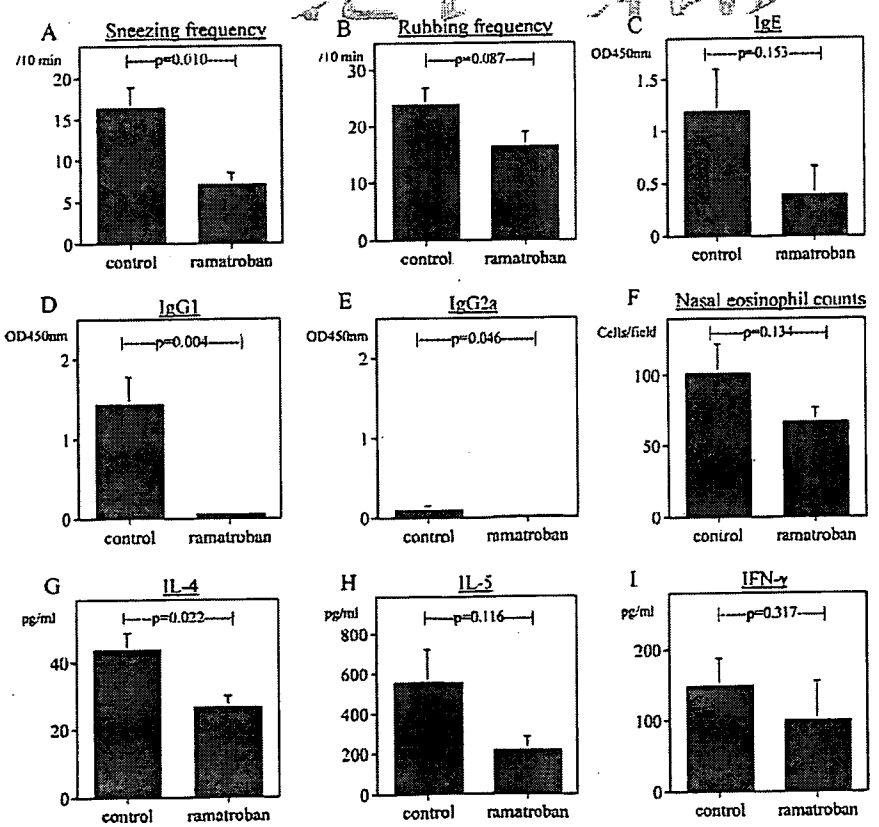

FIGURE 8. Effects of ramatroban on murine JCP. Ramatroban (30 mg/kg body weight), suspended in 5% methyl cellulose, was given orally once a day from 1 day before the first sensitization to the final challenge (day 0 to day 28). Control mice were given 5% methyl cellulose alone. After the final intranasal challenge, the frequencies of sneezing (*A*) and rubbing (*B*) were counted, and serum levels of Cry j 1-specific IgE (*C*), IgG1 (*D*), IgG2a (*E*), and nasal eosinophil count (*F*), as well as Cry j 1-induced IL-4 (*G*), IL-5 (*H*) and IFN-γ (*I*) were determined as described in *Materials and Methods*. Results are expressed as means ± SEM.

AQ: K

it is suggested that CRTH2-mediated pathway may induce pathology without regulating local production of these proinflammatory cytokines.

Outcomes of pollinosis were compared between sensitized/challenged CRTH2$^{-/-}$ mice and nonsensitized/single-challenged CRTH2$^{-/-}$ mice. The levels of Cry j 1-specific IgE (0.159 ± 0.044 vs 0 ± 0 OD at 450 nm: $p = 0.003$), Cry j 1-specific IgG1 (0.638 ± 0.163 vs 0 ± 0 OD at 450 nm: $p = 0.004$), nasal eosinophila (66.4 ± 8.2 vs 6.6 ± 1.1 cells/field: $p = 0.005$), and IL-4 production by submandibular lymph node cell (72.8 ± 31.1 vs 6.7 ± 3.8 pg/ml: $p = 0.004$) were significantly higher in sensitized and subsequently challenged CRTH2$^{-/-}$ mice as compared with nonsensitized and single-challenged CRTH2$^{-/-}$ mice. However, the frequencies of sneezing (1.7 ± 0.5 vs 0.6 ± 0.2 times in 10 min: $p = 0.088$) and rubbing (12.3 ± 2.6 vs 10.2 ± 3.1 times in 10 min: $p = 0.516$) were similar between two groups, suggesting that CRTH2 is particularly essential for the development of nasal symptoms.

Effect of ramatroban on Cry j 1-induced pollinosis

As seen in CRTH2-deficient mice, treatment with ramatroban significantly reduced several indicators of pollinosis including sneezing, Cry j 1-specific IgG1 production, and Cry j 1-induced IL-4 production by submandibular lymph node cells as compared with the control treatment (Fig. 8, *A*, *D*, and *G*). Although the differences did not reach to the statistical level, other parameters such as nasal rubbing, Cry j 1-specific IgE production, nasal eosinophilia, and Cry j 1-induced IL-5 production were also reduced by the treatment with ramatroban (Fig. 8, *B*, *C*, *F*, and *H*).

Discussion

In the present study, we analyzed the pathophysiological effects of nasal exposure to Cry j 1 in BALB/c mice. Mice sensitized with Cry j 1 without adjuvants showed not only allergic symptoms such as sneezing and rubbing but also produced Cry j 1-specific IgE and IgG1 and displayed nasal eosinophilia. Additionally, submandibular lymph node cells isolated from these mice produced IL-4 and IL-5 in recall response to Cry j 1. These results suggest that intranasal sensitization with Cry j 1 induces pollinosis in BALB/c mice.

To investigate the initiation of allergic rhinitis in vivo, administration of Ags via the natural route (i.e., through the nostril) is desirable. In fact, it is known that administration of Ags through different routes results in different degrees of IgE production (27, 28). Also, murine models of allergic rhinitis have been generated by intranasal or aerosol-mediated sensitization (8, 29), but these models generally employ adjuvants such as cholera toxin, which have immunoregulatory effects that may distort the physical sensitization (30, 31). Therefore, we and others have established murine models of allergic rhinitis by intranasal sensitization with Ags including *Schistosoma mansoni* egg Ag, phospholipase A_2 from honeybee venom, extracts of *Aspergillus fumigatus*, OVA, and trimellitic anhydride in the absence of adjuvants (5–7, 9, 32). We think that our current model is the first in which murine pollinosis was induced by intranasal sensitization with pollen allergen in the absence of an adjuvant. This model may be useful not only for understanding the pathophysiology of pollinosis but also for developing and/or testing new therapies for allergic rhinitis, especially JCP.

BALB/c mice sensitized with Cry j 1 showed an increase in the expression of CRTH2 mRNA in the nasal septum compared with control mice. This agrees with our recent report demonstrating that the amount of CRTH2 mRNA in nasal mucosa is significantly higher in patients with allergic rhinitis than in control subjects not showing hypertrophy of inferior turbinates (12). These results suggest that the expression of CRTH2 may play a role in the pathogenesis of allergic rhinitis both in humans and in mice. In fact, it is known that the expression of CRTH2 in eosinophils and CD4$^+$ T cells is elevated in atopic patients (33–35). CRTH2 is expressed by eosinophils and a subset of CD3$^+$ T cells in nasal mucosa, especially in patients with allergic rhinitis (23). Because a mAb against murine CRTH2 that can be used for immunohistochemistry is not currently available, we could not investigate the phenotype of cells expressing CRTH2 in mice.

The pathophysiology of allergic rhinitis was clearly impaired in CRTH2$^{-/-}$ mice. Following repeated intranasal sensitization and nasal challenge with Cry j 1, CRTH2$^{-/-}$ mice displayed reduced nasal symptoms, production of Cry j 1-specific IgE and IgG1, and nasal eosinophilia compared with WT mice. Additionally, submandibular lymph node cells from Cry j 1-sensitized CRTH2$^{-/-}$ mice produced significantly less IL-4 and IL-5 in response to Cry j 1 than those from WT mice. We think that the present results are the first demonstration of the in vivo role of CRTH2 in the initiation of Th2 responses in the upper airway.

We also found that Cry j 1-specific IgE and IgG1 but not IgG2a production was impaired in CRTH2$^{-/-}$ mice. Ag-specific IgE/IgG1 and IgG2a production is known to be positively regulated by Th2 and Th1 responses, respectively, in mice (36). Thus, our results indicate that signals mediated by CRTH2 selectively enhance Th2-type Ab production. The decreased production of IL-4 by submandibular lymph node cells from CRTH2$^{-/-}$ mice in response to Cry j 1 restimulation supports this result because IL-4 plays a critical role in IgE synthesis in vivo (37). Although whether CRTH2 activation directly leads to IL-4 production in mice remains unclear, recent investigations have demonstrated that PGD_2 causes the preferential induction of IL-4 production by Th2 cells in humans by binding to CRTH2 (38, 39). Additionally, our recent report showing that CRTH2 signals up-regulate CD40L in resting human Th2 cells supports our conclusions because the engagement of CD40 by CD40L is also essential for IgE isotype switching (39, 40).

After intranasal sensitization with Cry j 1, CRTH2$^{-/-}$ mice developed a weaker eosinophilia than did WT BALB/c mice. This suggests that CRTH2 mediates local eosinophil recruitment in this model, which agrees with reports showing that CRTH2 activation leads to changes in eosinophil shape, chemotaxis, and degranulation in vitro (16, 18, 41). Additionally, recent investigations have revealed that CRTH2 plays a proinflammatory role in eosinophil chemotaxis into inflamed tissue in vivo (11, 12, 21, 24, 42). On the other hand, submandibular lymph node cells from WT and CRTH2$^{-/-}$ mice produced similar amount of IL-5 after intranasal sensitization with Cry j 1. It is well known that IL-5 plays a critical role in eosinophilic inflammation, especially in mice (43). Although little is known about whether CRTH2 activation enhances IL-5 production in mice, CRTH2 activation on Th2 cells is known to induce IL-5 production in humans (38, 39). One explanation of why nasal eosinophilia was reduced in CRTH2$^{-/-}$ mice irrespective of IL-5 production is that cognate interaction between PGD_2 and CRTH2 on eosinophils may have an additive effect on local eosinophil recruitment, primarily due to the action of IL-5. In fact, in a mouse model of asthma, nebulized DK-PGD_2, a CRTH2 agonist, exacerbates eosinophilic lung inflammation without changes in IL-5 content in lung (21).

CRTH2$^{-/-}$ mice displayed a significantly lower frequency of both sneezing and nasal rubbing after the nasal challenge compared with the WT mice. Several molecules, including IL-5, CD80/CD86, H1, and CD39, have been shown to contribute to these symptoms via different mechanisms (38, 44–46). The present result suggests that activation of CRTH2 is also involved